



UNIVERSITAT POLITÈCNICA DE CATALUNYA  
BARCELONATECH

Escola d'Enginyeria de Barcelona Est

FINAL DEGREE THESIS

**Bachelor's Degree in Chemical Engineering**

**NANO-ENABLED COATINGS FOR PREVENTION OF MEDICAL  
DEVICE-RELATED INFECTIONS**



**Report and Annex**

**Author:** Emma Pubill Olivós  
**Supervisor:** Tzanko Tzanov  
**Department** Grup de Biotecnologia Molecular i Industrial  
**Co-supervisor:** Elaine Armelin Diggroc  
**Call:** 2023, June



## **Abstract**

Medical device (MD)-associated urinary infections are the most common healthcare related infections accounting for increased morbidity and mortality, and huge financial burden on healthcare systems. More than 80 % of such infections are due to biofilm formation, whereas approximately 40% of all nosocomial infections are catheter-associated urinary tract infections (CAUTIs). Strategies to reduce CAUTIs occurrence include frequent replacement of the device, which causes considerable discomfort to the patients and increases treatment costs, or aggressive antibiotic therapies with associated side effects such as hypersensitivity, inflammation and antimicrobial resistance (AMR) development. Therefore, innovative solutions for inhibition of bacterial growth and biofilm formation are needed to improve the catheters safety and long-term use, and patients comfort.

In this work, innovative Lauryl Gallate nanoparticles loaded with ceragenins (CGNPs), non-peptide mimics of antimicrobial peptides, with enhanced antibacterial activity and stability were developed in a single-step sonochemical process. CGNPs were then deposited on plasma-activated and preaminated with (3-aminopropyl) triethoxysilane silicone material together with antifouling zwitterions using high-intensity ultrasound coupled with laccase-mediated grafting to obtain stable coating for inhibition of biofilm formation. The developed nano-enabled coating proved to be effective against common Gram-negative and Gram-positive pathogens found in CAUTIs.

Additionally, the coated-silicone was characterized using FTIR-ATR spectroscopy and water contact angle. The results demonstrated that the generated coating could be used to control antibiotic-resistant biofilm-associated bacterial infections.

## Resum

Les infeccions urinàries associades a dispositius mèdics (MD) són les infeccions relacionades amb l'assistència sanitària més freqüents que representen un augment de la morbiditat i mortalitat i una gran càrrega financera per als sistemes sanitaris. Més del 80% d'aquestes infeccions es deuen a la formació de biofilm, mentre que aproximadament el 40% de totes les infeccions nosocomials són infeccions del tracte urinari associades al catèter (CAUTI). Les estratègies per reduir l'aparició de CAUTI inclouen la substitució freqüent del dispositiu, que causa molèsties considerables als pacients i augmenta els costos del tractament, o teràpies antibiòtiques agressives amb efectes secundaris associats com ara el desenvolupament d'hipersensibilitat, inflamació i resistència als antimicrobians (AMR). Per tant, es necessiten solucions innovadores per inhibir el creixement bacterià i la formació de biofilm per millorar la seguretat dels catèters i l'ús a llarg termini, i la comoditat dels pacients.

En aquest treball, es van desenvolupar nanopartícules innovadores de Lauryl Gallate carregades amb ceragenines (CGNP), imitacions no pèptids de pèptids antimicrobians, amb activitat i estabilitat antibacterianes millorades en un procés sonoquímic d'un sol pas. A continuació, els CGNP es van dipositar en material de silicona trietoxisilà activat per plasma i preaminat amb (3-aminopropil) juntament amb zwitterions antifouling mitjançant ultrasò d'alta intensitat juntament amb empelt mediat per lacasa per obtenir un recobriment estable per inhibir la formació de biofilm. El recobriment desenvolupat amb nano-habilitat va demostrar ser eficaç contra els patògens Gram-negatius i Gram-positius comuns que es troben en CAUTIs.

A més, la silicona recoberta es va caracteritzar mitjançant l'espectroscòpia FTIR-ATR i l'angle de contacte amb l'aigua. Els resultats van demostrar que el recobriment generat es podria utilitzar per controlar les infeccions bacterianes associades a biofilms resistents als antibiòtics.

## Resumen

Las infecciones urinarias asociadas a dispositivos médicos (MD) son las infecciones más comunes relacionadas con la atención médica y representan una mayor morbilidad y mortalidad, y una enorme carga financiera para los sistemas de atención médica. Más del 80 % de estas infecciones se deben a la formación de biopelículas, mientras que aproximadamente el 40 % de todas las infecciones nosocomiales son infecciones del tracto urinario asociadas al catéter (ITUAC). Las estrategias para reducir la aparición de CAUTI incluyen el reemplazo frecuente del dispositivo, lo que causa una incomodidad considerable a los pacientes y aumenta los costos del tratamiento, o terapias agresivas con antibióticos con efectos secundarios asociados, como hipersensibilidad, inflamación y desarrollo de resistencia antimicrobiana (AMR). Por lo tanto, se necesitan soluciones innovadoras para la inhibición del crecimiento bacteriano y la formación de biopelículas para mejorar la seguridad y el uso a largo plazo de los catéteres y la comodidad de los pacientes.

En este trabajo, se desarrollaron innovadoras nanopartículas de galato de laurilo cargadas con cerageninas (CGNP), imitadores no peptídicos de péptidos antimicrobianos, con actividad antibacteriana mejorada y estabilidad en un proceso sonoquímico de un solo paso. Luego, los CGNP se depositaron en material de silicona de trietoxisilano (3-aminopropil) activado por plasma y preaminado junto con iones de zwitter antiincrustantes usando ultrasonido de alta intensidad junto con injerto mediado por lacasa para obtener un recubrimiento estable para la inhibición de la formación de biopelículas. El recubrimiento nanohabilitado desarrollado demostró ser eficaz contra los patógenos gramnegativos y grampositivos comunes que se encuentran en las CAUTI.

Además, la silicona recubierta se caracterizó mediante espectroscopia FTIR-ATR y ángulo de contacto con el agua. Los resultados demostraron que el recubrimiento generado podría usarse para controlar infecciones bacterianas asociadas a biopelículas resistentes a los antibióticos.



## Appreciations

In the first place, I would like to dedicate this space to Professor Tzanko Tzanov for this opportunity, for trusting me to participate in this project, and Kristina Ivanova and Antonio J. Puertas too, for the incredible dedication and patience that they had had in me since the beginning of this challenge. Eternally grateful to them and to the GBMI colleagues for the fullness lived during these months. Also to Elaine for being a great teacher and person, she has been an incredible backbone during my degree.

I would like to thank, from the beginning and until the end, my parents for giving me the lucky life that I have and being the ones who have suffered and lived every moment of this race to the full. Especially to my brother Pau, for being the inspiration for the essence of life, for self-improvement and for the researcher that I want to become to help, facilitate and defend the vital rights of all.

To all my life and career partners for having grown up with me and for having decided to love me even in my worst moments. To Marina Roustan, for the light she has brought to my life.

And finally, I want to thank the past for blindly leading me to this experience and being able to value it. Regain faith in me.







## Glossary

ADME	Absorption, Distribution, Metabolism, Excretion
AHL	Acyl Homoserine Lactones
AIQ	Autoindicators of Quorum
AMR	Antimicrobial Resistance
APTES-S	Pre-treats Silicone
CAUTI	Catheter-Associated Urinary Tract Infections
CGNP	Ceragenin in Lauryl Gallate Nanoparticle
CGNP-S	CGNP Coating Silicone
CSA	Ceragenin: Antimicrobial Cathodic Steroids
EPM	Extracellular Polymeric Matrix
FTIR	Spectrophotometer
HAI	Healthcare Associated Infections
HGT	Horizontal Gene Transfer
HYB-S	CGNP and Sulfobetaine Coating Silicone
MBC	Minimum Bactericidal Concentration
MIC	Minimum Inhibitory Concentration
NPs	Lauryl Gallate Nanoparticle
PDMS	Polydimethylsiloxane
PEP	Peptide Solution
QS	Quorum-Sensing

ROS            Reactive Oxygen Species

SEM            Scanning Electron Microscope



## List of Figures

<i>Figure 1. Representation of the four stages of biofilm formation established until now.</i>	4
<i>Figure 2. Representation of horizontal gene transfer between bacteria.</i>	5
<i>Figure 3. Representation of the biofilm formed in a urinary catheter.</i>	6
<i>Figure 4. Types of polymeric medical devices associated with nosocomial infections.</i>	7
<i>Figure 5. Representation of a nanoparticle with a biochemical interface. This combination improves the properties that the particle is intended for.</i>	9
<i>Figure 6. Representation of nanoparticles formation designed as nanovesicles from the emulsion of two liquids, to contain a product encapsulated in a monolayer of the other product.</i>	9
<i>Figure 7. Representation of the molecular structure of the nowadays most functional ceragenins. Its design is based on the structure of the polyxime B protein, as can be seen. The characteristic of each ceragenin is a function of the functional groups attached to that structure.</i>	10
<i>Figure 8. Table of the different equipment used to carry out the experimental process of the project.</i>	13
<i>Figure 9. Table of the different compounds used to carry out the synthesis of the nanoparticles and the coating of the silicones, and description of their role in the process.</i>	14
<i>Figure 10. Table of the different reagents has been used to characterize and antimicrobial and antibiofilm properties evaluation of each processed sample.</i>	15
<i>Figure 11. Table of the different bacteria that have been used to evaluate the synthesized samples</i>	15
<i>Figure 12. Table of the different media necessary to be able to carry out the bacterial culture for the antimicrobial and antibiofilm tests.</i>	15
<i>Figure 13 Table of the values obtained from the DLS and the Z Potential, for each of the CGNP variants using</i>	21
<i>Figure 14 Calibration curve built using DMSO as a standard and the absorbance values obtained for different concentrations of CGNPs. Samples were prepared with 40 mg/mL initial CSA-131. Concentration was only analysed.</i>	22

<i>Figure 15. Calibration curve built using gallic acid as a standard and the absorbance values obtained for different concentrations of CGNPs. Samples were prepared with 40 mg/mL initial CSA-131. Concentration was only analysed.....</i>	<i>22</i>
<i>Figure 16. SEM images of CGNPs (left). Histogram of CG NPs size distribution based on the total count using ImageJ software (right).....</i>	<i>23</i>
<i>Figure 17. Representation of the antioxidant activity of CGNPs and NPs. Its reducing capacity does not decrease until dilution 1:1,000,000. ....</i>	<i>24</i>
<i>Figure 18. A) P. aeruginosa, B) S. aureus and C) E. coli growth (%) after 24 h incubation with CG NPs at different concentrations.....</i>	<i>26</i>
<i>Figure 19. S. aureus and P. aeruginosa growth (%) after 24h h incubation with CG NPs.....</i>	<i>26</i>
<i>Figure 20. Representation of the effect of CGNP and NP on the metabolism of Grampositive and Gramnegative bacteria.....</i>	<i>28</i>
<i>Figure 21. E. coli and S. aureus biofilm growth (%) after 24h h incubation with CG NPs.....</i>	<i>29</i>
<i>Figure 22. ATR–FTIR spectra of each sample of silicone.....</i>	<i>31</i>
<i>Figure 23. Representation of the silicone hydrophilicity character as it is treated, with photos of the drop reaction once it falls on the surface. ....</i>	<i>32</i>
<i>Figure 24. Images taken from the microscope of the qualitative amount of protein adhered to the surface of the different silicones. ....</i>	<i>33</i>
<i>Figure 25. Representation of P. aeruginosa and S. aureus biofilm growth (%) after 24h h incubation with each silicone sample. ....</i>	<i>34</i>
<i>Figure 26. Live/Dead assay images of S. aureus cultures in the four types of silicone sample. They are not consistent. ....</i>	<i>35</i>
<i>Figure 27. Live/Dead assay images of P. aeruginosa cultures in the four types of silicone sample. They are not consistent. ....</i>	<i>36</i>
<i>Figure 28. Diagram of three phases of the environmental impact with the misuse of reagents.....</i>	<i>38</i>
<i>Figure 29. Diagram of three phases of the environmental impact with the misuse of bacteria.....</i>	<i>38</i>
<i>Figure 30. The amounts of carbon dioxide generated during the process. ....</i>	<i>39</i>

Figure 31. Table of the resulting costs of each proposed section, plus the total cost of the experimental nanoparticle coating process. ....42

Figure 32. Table of the different compounds used for this experimental process with their prices and sales quantities. The cost proportional to the used fraction of each one has been calculated. ....43

Figure 33. Table of costs of the material and equipment required to carry out each of the assays and synthesis. 43

Figure 34. Table about the overall cost of working time, including experimental work and its subsequent analysis, such as bibliography research .....44

# Index

<b>ABSTRACT</b>	<b>III</b>
<b>RESUM</b>	<b>IV</b>
<b>RESUMEN</b>	<b>V</b>
<b>APPRECIATIONS</b>	<b>VII</b>
<b>1. PREFACE</b>	<b>1</b>
1.1. Background and Motivation	1
1.2. Requirements	1
<b>2. INTRODUCTION</b>	<b>3</b>
2.1. Antibiotic Resistance Threat	3
2.2. Bacterial Biofilm Formation on Medical Devices	4
2.2.1. Mechanisms of bacterial adhesion	4
2.2.2. Mechanisms of bacterial resistant	5
2.2.3. Medical devices-related infections	6
2.3. Strategies against biofilm formation on urinary catheters	7
2.3.1. Zwitterionic Materials	8
2.3.2. Nanoformulated Matrix-Degrading Enzymes	8
2.4. Nanotechnology	8
2.5. Ceragenins: Synthetic mimics of antimicrobial peptides	10
2.6. Objective	10
2.7. Scope	11
<b>3. MATERIAL</b>	<b>13</b>
3.1. Instrumentation	13
3.2. Reagents	14
3.3. Bacterial and Medium	15
<b>4. METHODOLOGY</b>	<b>16</b>
4.1. Nanoparticles synthesis	16
4.1.1. NPs Characterization	16
4.1.2. Quantification of Total Phenolic Content (TPC)	16
4.1.3. Determination of CSA-131 concentration in the NPs	16
4.1.4. Minimum Inhibitory (MIC) and Bactericidal Concentration (MBC) of the NPs	17

4.1.5.	Metabolic Activity of bacteria in presence of the NPs.....	17
4.1.6.	Antibiofilm activity of the NPs: Cristal Violet Assay .....	17
4.1.7.	Antioxidant Capacity .....	18
4.2.	Sono-enzymatic coating of silicone catheters .....	18
4.2.1.	Silicone Coating with antibacterial NPs by Sono-enzymatic Approach .....	18
4.2.2.	Surface characterisation.....	19
4.2.3.	Determination of the hydrophilic property .....	19
4.2.4.	Protein Adsorption .....	19
4.2.5.	Antimicrobial activity of NP coated silicone.....	19
4.2.6.	Antibiofilm activity.....	20
4.2.7.	Live/Dead Kit Assay .....	20
<b>5.</b>	<b>RESULTS AND DISCUSSION</b> .....	<b>21</b>
5.1.	Nanoparticles Characterisation .....	21
5.1.1.	DLS and Z potential.....	21
5.1.2.	CSA Quantification.....	21
5.1.3.	Quantification of Total Phenolic Content (TPC).....	22
5.1.4.	Scanning Electron Microscope .....	23
5.1.5.	Antioxidant activity.....	23
5.1.6.	Antimicrobial activity of the nanoparticle properties.....	24
5.1.7.	Metabolic Activity of Bacteria .....	28
5.1.8.	Antibiofilm Activity of CGNPs.....	28
5.2.	Sono-enzymatically Enzymatically Triggered Bottom-Up functionalization of silicones .....	30
5.2.1.	Characterisation of the nano-enabled coating .....	30
5.2.2.	Water Contact Angle Measurements .....	32
5.2.3.	Initial Protein Attachment.....	33
5.2.4.	Antimicrobial activity of nano-enabled silicone.....	34
5.2.5.	Live/Dead Kit Assay .....	35
<b>6.</b>	<b>ENVIRONMENTAL STUDY</b> .....	<b>37</b>
6.1.	Environmental Impacts of the Experimental Phase .....	37
6.2.	Environmental Impact of Production and Product .....	39
6.3.	Environmental Impact Due to Energy Consumption .....	39
<b>7.</b>	<b>CONCLUSIONS</b> .....	<b>41</b>
<b>8.</b>	<b>ECONOMIC ANALYSIS</b> .....	<b>42</b>
8.1.	Reagents and products .....	42

8.2. Equipment and material.....	43
8.3. Staff.....	44
<b>9. REFERENCE</b> .....	<b>45</b>

---



# 1. Preface

## 1.1. Background and Motivation

The *Molecular and Industrial Biotechnology Group* (GBMI) is a multidisciplinary research group part of the *Chemical Engineering Department* of the Polytechnic University of Catalonia (UPC). Located at the GAIA research centre in Terrassa, it is comprised of two teams who work in parallel lines of research, the molecular and the applied. In the first case, the *Molecular Biotechnology Team's* main field of study evolves around the structure and molecular properties of proteins, to combat-related conditions.

In contrast, the *Applied Biotechnology team* focuses on the industry by developing new products and technologies. They work with both national and international partners to research and provide innovative solutions within the field of bioengineering, improving the efficiency of processes and materials, as well as some of the already registered patents.

Some of the approaches include bioprocesses, functional textiles, cosmetic formulations, or nano/micro drug delivery systems, among others. The aim is to integrate biology in this sector as an essential element for the development of new applications.

Considering the context around pharmaceuticals and antibiotic resistance, antimicrobial strategies using new synthesis techniques have only recently been researched. As the latest addition to this year's research, the use of ceragenin, non-peptide mimics of the antimicrobial peptides with improved stability and activity, is being studied to develop new nanoformulations and coatings for MDs.

## 1.2. Requirements

This final degree project is part of the GBMI ongoing research on the application of ceragenins for engineering nanomaterials that inhibit bacterial growth and biofilm formation. Prior to the realization of this project, it is worth mentioning all the progress made by the Applied Biotechnology Team in the creation of materials that provide the basis for further innovation with new ideas, serving as the foundation for this project, such as ***the Multimodal silver-chitosanacylase nanoparticles inhibit bacterial growth and biofilm formation by Gram-negative Pseudomonas aeruginosa bacterium*** [1], or ***Nanomaterials and Coatings for Managing Antibiotic-Resistant Biofilms*** [2], where they design new nanocomposites as a solution to inhibit bacteria and their biofilms.

Thus, ***Nanoparticle coatings for prevention of medical device-related infections*** is a continuation of the work started by the PhD student Antonio Jesús Puertas Segura member of the

applied biotechnology team, on new techniques for nanoparticles synthesis and silicone functionalization. More precisely, the surfactant-based nanoemulsion creates vesicles formed by an antioxidant compound, where ceragenin will be encapsulated for urinary tract infection prevention techniques, drawn from the PhD thesis of Dra. Kristina Dimitrova Ivanova.

## 2. Introduction

### 2.1. Antibiotic Resistance Threat

In May 2016, economist *Jim O'Neil* published an 84-page review on antimicrobial resistance (AMR), which had worldwide repercussions, as it ruled out a situation that years ago was under rumors and that with previous notice, nobody acted upon it. It is about the bacterial genome that, as we are aware, is becoming resistant to the antibiotics that have been deliberately distributed. Alexander Fleming already warned about the current repercussions. In 1945, he stated; *"A day will come in which anyone will be able to buy penicillin. Because of it, there will be the danger that an ignorant man can easily take an insufficient dose and expose their microbes to non-lethal amounts that can, in contrast, make them more resistant."*

In 2016, it was causing around 700.000 deaths per year along with a predicted exponential growth of 10 million by 2050. If a solution is not found, it will come at the cost of losing 2 billion dollars per year. For decades, we have immersed ourselves in idyllic immunity by trusting the same antibacterial molecules that were once created, while turning a blind eye to discover new ones [3].

Bacteria is the longest-lived in the biosphere, this counterattack is a mechanism that should not come as a surprise. It has developed the fascinating capacity to evolve and adapt to its habitat along with the external factors that surround it. This is because its genome is constantly updated when information is equally fissioned. Hence the resistance to antibiotics.

In addition, bacteria communicate with each other, functioning as a hive mind. It consists of a significant virulence factor since it protects them from any antimicrobial stress, developing infections with highly difficult cures. This situation becomes most notable in clinical situations where the patient, due to health issues, lives surrounded by permanent or momentary medical devices that imply a large focus of attention.

Currently, the most feasible way to revert this situation is the creation of new strategies through biotechnology to create new antibacterial and antifouling methods, as a way to change the use of biocides that increase antibiotic resistance.

## 2.2. Bacterial Biofilm Formation on Medical Devices

### 2.2.1. Mechanisms of bacterial adhesion

Bacteria share a communications system called quorum-sensing (QS), that allows them to regulate the expression of genes depending on the bacteria's density. When a small group of bacteria settles, they secrete a range of extracellular substances to form a extracellular polymeric matrix (EPM) that will allow them adhere to the surface and facilitate the transfer of nutrients and chemical signals such as autoinducers (AIs) between bacteria to generate QS and coordinate in order to form biofilm. The AIs move through the matrix, and they are specific for each type of bacteria; for the Gram-negatives they are acyl homoserine lactones (AHL) and for Gram-positives they are auto indicator peptides (AIPs). When they assemble and reach the critical threshold, they are detected by the surrounding bacteria through quorum-sensing, expressing their genes for the formation of biofilms and the production of virulence factors [2].

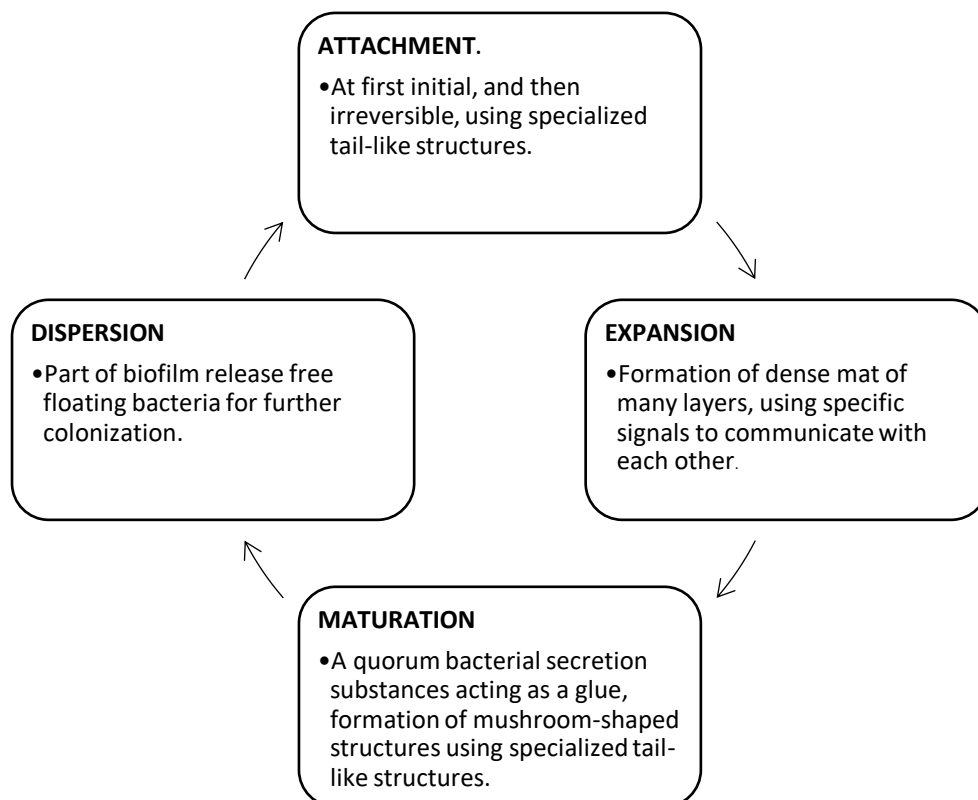


Figure 1. Representation of the four stages of biofilm formation established until now.

In addition, biofilms are part of the coordinated colonies that generate a densely populated closed system that protects and reduces the diffusion of drug molecules, while the biofilm's intimate surroundings offer excellent conditions for allowing horizontal gene transfer along with resistance

development. Such enhanced virulence makes around 1,000 times more aggressive and resistant than planktonic microorganisms in their environment [1].

## 2.2.2. Mechanisms of bacterial resistant

The antibiotic resistance focuses on  $\beta$ -lactam antibiotics, including penicillin, amoxicillin, ampicillin, and ceftriaxone [4]. Some of the bacteria biosynthesize this component to interfere with the synthesis of the bacterial cell wall of opponent species, weakening them or causing their death. A prominent example is the case of the Penicillium. The extended use of this antibiotic has allowed bacteria to reproduce it with a wider spectrum of effectiveness, becoming stronger than the current antibiotics, due to the genetic mutations originating from the survival of a resistant bacteria.

These mutations result from the HGT (Horizontal Gene Transfer), a genetic transfer process that allows the exchange of genetic material without the need to procreate or have direct descendants. It takes place both between them, and among other species and genders.

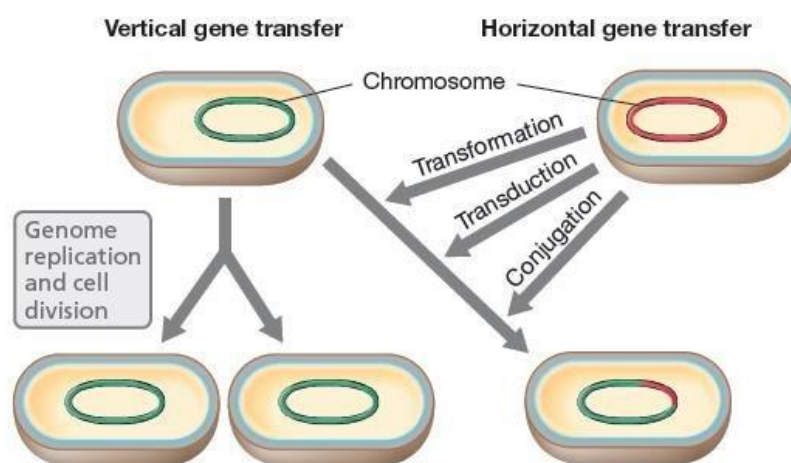


Figure 2. Representation of horizontal gene transfer between bacteria.

Therefore, the bacteria adjacent to the resistant bacteria obtain the other bacteria resistance genes, often called integrons. They contain integrase, an enzyme that allows them to capture and incorporate the new resistance genes into their structure.

Another defence mechanism relies on the answer to oxidative stress. Bacteria secrete antioxidants that neutralize the existing free radicals in their environment in order to protect themselves. Moreover, they also produce reactive oxygen species (ROS), as metabolic by-products of aerobic respiration or when they are in touch with reactive species, and thus, unbalance the bacteria's metabolism, generating free radicals.

### 2.2.3. Medical devices-related infections

For years, medical technology has used biocompatible polymers to elaborate surgical instruments, either post-operation or permanent.

Its extended use offers perfect conditions for bacteria proliferation and the formation of biofilm, by being in a moisturizing atmosphere, such as a wound, which offers a substrate for colonies because of the adsorption of non-specific proteins in the silicone, forming a conditioning layer. The material characteristics favour the exchange of substances, acting as a source of the substrate to retain proteins, directly influencing the metabolism and, as a consequence, the biofilm's reactions. Furthermore, the exchange of signals of the quorum-sensing system, by participating the surface of the material with the interactions that take place in the EPM. Its hydrophobic properties lead to a strong attraction for the biofilm while facilitating its adhesion and hindering the penetration of antimicrobial agents such as medicines or the immune system.

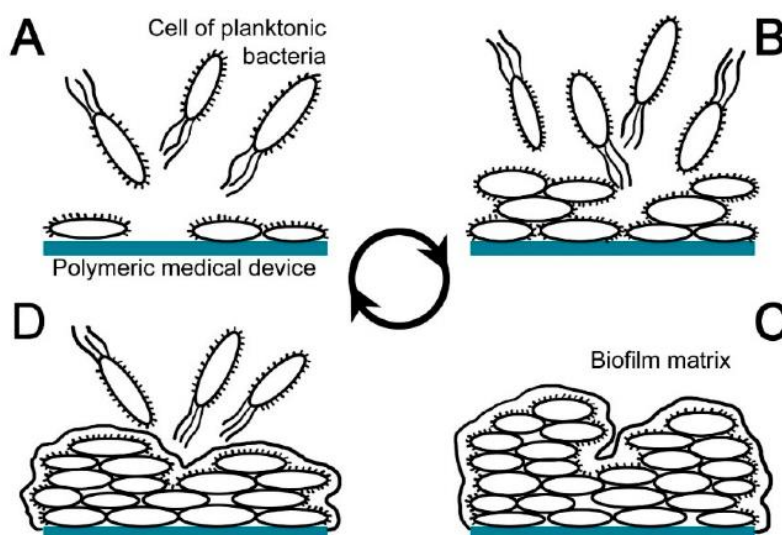


Figure 3. Representation of the biofilm formed in a urinary catheter.

A high bacteria resistance risk has been generated when trying to fight against this situation with postoperative antibiotic therapy to reduce the frequency of the infections such as morbidity and mortality. Nonetheless, problems have increased by giving bacteria the opportunity to mutate until achieving *Staphylococcus aureus*, which is resistant to methicillin and vancomycin, or *Enterococcus* which is resistant to vancomycin and extended-spectrum  $\beta$ -lactamase-producing gram-negative bacilli. Nowadays, these nosocomial infections are very difficult to treat [5].

700.000 people pass away each year due to common illnesses, currently untreatable in most cases due to risky complications such as sepsis or septic shock. The most common infections are those related to catheters caused by *Pseudomonas aeruginosa* and *Escherichia coli*.

Microbial Species	Medical Devices	Examples
<i>Staphylococci, Enterobacteriaceae, Enterococci and Candida species</i>	Catheters	Blood vessel catheter, CAPD catheters
	Tubes	Cerebrospinal fluid shunts, endotracheal tubes
	Cardiological implants	Arterial grafts, cardiac valves, pacemaker electrodes, total artificial hearts
<i>Enterobacteriaceae and Enterococci</i>	Prostheses	Total joint replacements (endoprostheses), ocular and penile prostheses
	Urinary catheters	Transurethral, suprapubic, and nephrostomy catheters,
	Urinary stents	Double-J stents

Figure 4. Types of polymeric medical devices associated with nosocomial infections.

Within the group of Healthcare Associated Infections (HAI), those with a urinary tract nature caused by the urinary catheters (CAUTI) tend to be the most common, accounting for 80% of treatable cases. Catheter-associated urinary tract infections (CAUTIs) are amongst the most common HAIs, accounting for 80% of urinary tract infections currently treated in hospitals [6].

### 2.3. Strategies against biofilm formation on urinary catheters

Despite the aforementioned, innovation is being made in the field of biotechnology with the aim to propose new paradigms and hybrid strategies to respond to antibiotic resistance. These solutions will start from the need to create something that could eradicate bacteria avoiding the appearance of new resistance mechanisms. Meaning that it shall not be invasive but rather something natural that poses an alternative to the abuse of antibiotics and medication [7].

The anti-adhesive strategy is the prevention of EPM formation by avoiding contact of the bacteria with the surface or its anchoring components, thus preventing AIQ, AIP and substrate transport. Some of the new application techniques are hydrophilic materials or their coating.

### 2.3.1. Zwitterionic Materials

They are materials that have equimolarly the same positive and negative charge distributed homogeneously throughout the chain of the material, which allows the union of water molecules, making the material hydrophilic and without optimal conditions for the anchoring of the EPM, based on the non-specific interaction of the proteins that make it up [8].

### 2.3.2. Nanoformulated Matrix-Degrading Enzymes

Matrix-degrading enzymes target the extracellular components secreted by bacteria during biofilm formation. Degrading the biofilm adhesive structure by different enzymes such as  $\alpha$ -amylase, alginate lyase, proteases, and deoxyribonucleases (DNases) is a feasible strategy to weaken biofilms and increase the bacterial susceptibility to antibacterial agents.  $\alpha$ -amylase is a glycoside hydrolase that catalyzes the breaking of  $\alpha$ -1,4-glycosidic bonds. Its main substrate is starch; however, it also acts on several carbohydrates present in the biofilm matrix [9].

## 2.4. Nanotechnology

Nanotechnology is the development of nanoscale objects of materials, devices, and systems that, thanks to their dimensions, provide advantages in fields such as biology -due to their higher surface-to-volume ratio-, favoring interactions with their environment. Their small volume provides improved properties in proportion to their larger versions due to their compact structure.

The use of nanotechnology as a new therapeutic approach ables the design of new methods with high efficacy, by providing improved pharmacokinetics [10] in the ADME stages. That is to say, the relationship between the antimicrobial and the patient during the process of absorption, distribution, metabolization, and elimination of the substance by being an alternative to drug dosing, should always be monitored.

On one hand, metallic nanoparticles are the most studied, as they facilitate interactions due to their electromagnetic potential, resistance to biodegradation, and cross barriers that are impermeable to each other. On the other hand, this generates a secondary effect, as it forms holes by the electrostatic effect in an unspecified way and can therefore be in the membranes of any cell when exposed for a prolonged period of time. In addition, its ions can be deposited in organs and cell walls, causing cytotoxicity, genotoxic and carcinogenic actions. But, in order to interact with a microorganism, the nanoparticle must be coated with some organic compound as a biochemical interface [11].



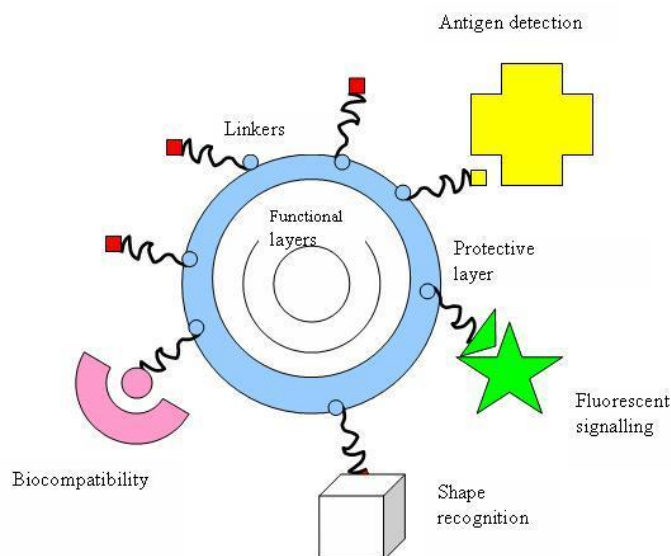


Figure 5. Representation of a nanoparticle with a biochemical interface. This combination improves the properties that the particle is intended for.

Nanoemulsions are particles found in a colloidal system used for drug transport. They are amorphous spheres that replace vesicles and house the antibiotic inside, improving the bioavailability of the drug and therefore the therapeutic efficiency of the drug, minimizing adverse effects and toxic reactions.

Its formulation can be done by many methods, but the most efficient one is ultrasonic emulsification. When the sonicator comes into contact with liquid, it produces a mechanical vibration that generates vapor cavities with the medium, favouring a collapse of bubbles that implode. This process is referred to as cavitation. To do so, a surfactant is used to stabilize the particles formed in the emulsion by cavitation, creating a monolayer that encapsulated the hydrophobic material inside it to produce nanoparticles. As it reduces surface tension, it prevents the agglomeration of nanoparticles [12].

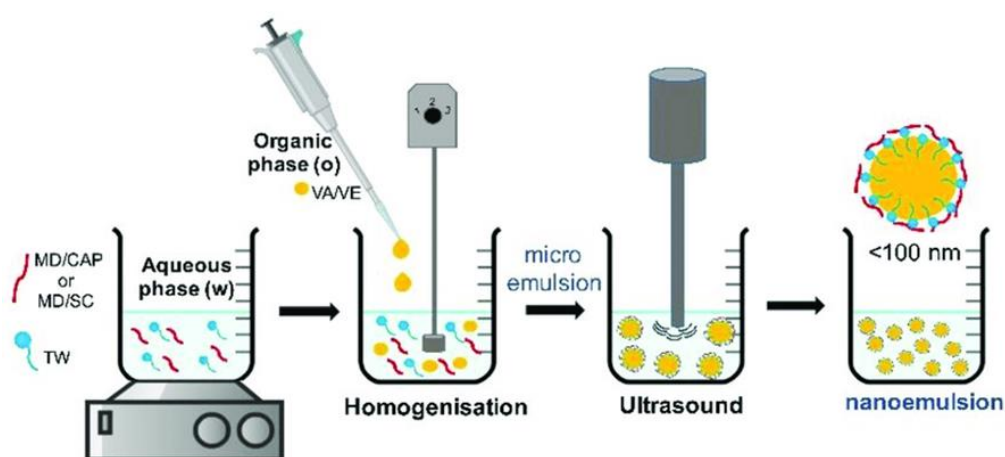


Figure 6. Representation of nanoparticles formation designed as nanovesicles from the emulsion of two liquids, to contain a product encapsulated in a monolayer of the other product.

## 2.5. Ceragenins: Synthetic mimics of antimicrobial peptides

The key to the immunology of species against pathogens are the antimicrobial peptides (AMP) that are found on the surface of the mucous membranes and organs in the first line of attack. Its structure is both catatonically charged and amphiphilic, providing a great selectivity towards the membranes of the microorganism -due to its opposite charge-, affecting the balance of the membrane and, as a consequence, the death of the cell. On the contrary, they are highly sensitive to the proteolytic enzymes (proteases) that break down and process the proteins of the living species, as well as the changes in pH. Because of this reason, its medical application is fading due to the costs involved in their sintering on therapy against diseases.

As an alternative, ceragenins (CSA) have been developed based on the most researched AMP structural model, polyximide B. In order to reproduce the same characteristics (in both cationic and amphiphilic character) they have been synthesized with amines and cholic acid.

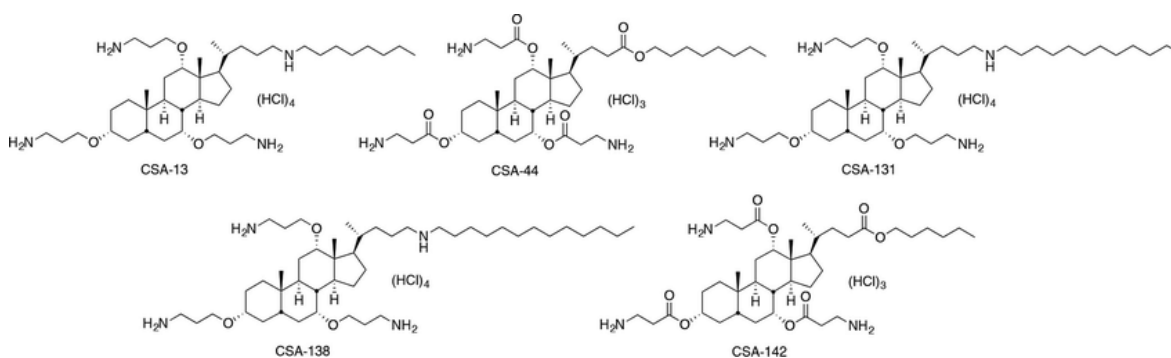


Figure 7. Representation of the molecular structure of the nowadays most functional ceragenins. Its design is based on the structure of the polyxime B protein, as can be seen. The characteristic of each ceragenin is a function of the functional groups attached to that structure.

Furthermore, they have a broad spectrum against both bacteria by having antibiofilm and antimicrobial potential. That is to say, there are different types of CSA, such as CSA-131. Biodistribution studies have highlighted that they do not accumulate in the organism, but they are rather eliminated with urine and bile acids. In addition, it helps to restore the microenvironment of the affected area with its unfavorable biophysical characteristics for the type of bacteria that is designed to be bactericidal, as they are very selective. CSA-131 causes high oxidative stress, and several studies support its use in the treatment of urinary tract infections. Nonetheless, due to the novelty of this product, in vitro studies have not yet been performed in vivo.

## 2.6. Objective

The main objective is to developed antifouling, antibacterial and antibiofilm nano-enabled coating on silicone catheters to prevent CAUTIs. The following specific objectives define the roadmap towards the

generation of highly efficient nanocoating that will eradicate bacteria and inhibit the establishment of antibiotic resistant biofilm:

- Nanoformulation of ceragenins using high intensity ultrasound.
- Sono-enzymatic coating of silicone catheters with CSA NPs and zwitterions
- Characterization the resulting nano-enabled coating.
- *In vitro* evaluation of the antifouling, antibacterial and antibiofilm potential of the generated coatings against common pathogens.
- Decision of the best performing approach and whether the combination between the CSA NPs and zwitterions in the same coatings is effective.

## 2.7. Scope

With this project, is it hoped to develop a hybrid nanocoating on silicones, pretreated with X with the purpose of Y. The coating is created by combining the synthesized nanoparticles with sulfobetaine, in order to impart improved antibacterial and antibiofilm activities in the generated layer caused by the zwitterionic charge as a way to stabilize the nanoparticles so that they do not agglomerate and, as a result, poorly coat the surface. The combination is done via the enzymatic action of the laccase as oxidoreductase, which will be added in the reaction mixture during the surface functionalization of the silicone by means of the impact force generated by the acoustic cavitation of an ultrasonicator.

Previously, nanoparticles are synthesized with the same method, a liquid emulsification based on Tween 80 as a surfactant by the implosion of bubbles generated by ultrasonication. The aim is to create vesicles of Lauryl Gallate as an antioxidant agent and prevent the ROS effect of bacteria and encapsulate the CSA-131 ceragenins. By doing so, it is achieved a slow release of the antimicrobial agent as the nanoparticles oxidize. Finally, the goal is to characterize both zoned parts and evaluate the antimicrobial and anti-adherent properties by incubating the samples in cultures of Gram-negative *P. aeruginosa* and *E. coli* bacteria and Gram-positive *S. aureus* bacteria.

### 3. Material

#### 3.1. Instrumentation

Equipment	Brand/Model	Remarks
<i>Centrifuge</i>	Alresa	<ul style="list-style-type: none"> <li>- Fixed angle rotor of 30 degrees</li> <li>- Maximum speed up to 6.000 rpm</li> <li>- Permits use of up to 24 microtubes of 2.2 mL</li> </ul>
<i>Zetasizer Nano Z</i>	Malvern Instruments	<ul style="list-style-type: none"> <li>- Dedicated to zeta potential measurement</li> </ul>
<i>Contact Angle and Surface Free energy measuring device</i>	Drop-Shape analyzer DSA 25 (Krüss)	<ul style="list-style-type: none"> <li>- Characterization of chemically or physically functionalized surfaces.</li> <li>- Testing wettability of different materials: glass, plastic, ceramic.</li> <li>- Surface free energy from contact angle</li> <li>- Static and dynamic contact angle determination</li> </ul>
<i>FTIR spectrophotometer</i>	Perkin Elmer / FTIR Spectrum 100R	<ul style="list-style-type: none"> <li>- UATR</li> <li>- Suitable for film, powder, and solubilised samples</li> </ul>
<i>Incubator 37 °C</i>	Sanyo MIR-262 model	<ul style="list-style-type: none"> <li>- Effective size: 153 L</li> <li>- 6 shelves support</li> <li>- Temperature control range: from 5 °C to 60 °C</li> <li>- Electronic timer with delay timer</li> <li>- Digital display</li> </ul>
<i>Multiwell plate reader</i>	Tecan /Infinite M200	<ul style="list-style-type: none"> <li>- Fluorescence</li> <li>- UV-Vis</li> <li>- Luminiscence and dual luminiscence</li> </ul>
<i>Fluorescence Microscope</i>	NIKON / Eclipse Ti-S	

Figure 8. Table of the different equipment used to carry out the experimental process of the project.

## 3.2. Reagents

The description of each compound is the role it has within the experimental process.

Experimental Compounds	Description
<i>DMSO</i>	Amphiphilic solvent, interact with both polar and nonpolar substances.
<i>Lauryl Gallate</i>	Antioxidant agent of amphiphilic nature.
<i>Tween 80</i>	Surfactant, reduces the surface tension between two phases and stabilizes the colloidal system.
<i>Ethanol</i>	Polar Solvent
<i>Mili-Q water</i>	High Purity Water
<i>Sulfobetaine</i>	Zwitterionic surfactants, prevent protein attachment facilitating polar union such as water
<i>Laccase</i>	Oxidoreductase enzyme, oxidizes phenols among others
<i>Sodium Acetate</i>	pH regulator

Figure 9. Table of the different compounds used to carry out the synthesis of the nanoparticles and the coating of the silicones, and description of their role in the process.

Reagents	Description
<i>Gallic Acid</i>	Phenol acid with antioxidant property, for the comparison of oxidative stress with the samples
<i>Folin-Ciocalteu</i>	Quantification Phenols Reagent
<i>Fluorescamine</i>	Powder, used for detection of primary amines.
<i>Crystal Violet</i>	Stain for Histological Staining
<i>Resazurin</i>	Metabolic Indicator

<i>DPPH</i>	Oxidation Indicator
<i>FTIC-BSA</i>	Combination of fluorescent dye (FITC) and protein (BSA) for the protein attachment assay
<i>Live/Dead Kit Assay</i>	Fluorescent dyes for viability assays,

Figure 10. Table of the different reagents has been used to characterize and antimicrobial and antibiofilm properties evaluation of each processed sample.

### 3.3. Bacterial and Medium

Bacteria Name	Description
<i>Staphylococcus aureus</i>	Gram-positive bacteria
<i>Pseudomonas aeruginosa</i>	Gram-negative bacteria
<i>Escherichia coli</i>	Gram-negative bacteria

Figure 11. Table of the different bacteria that have been used to evaluate the synthesized samples

Medium Name	Description
<i>Nutrient Broth</i>	Nutrient Medium for Antibiofilm Assays
<i>Mueller Hilton Broth</i>	Nutrient Medium for Antimicrobial Assays
<i>Tryptic Soy Broth</i>	Nutrient Medium for Antibiofilm Assays
<i>Phosphate Buffered Saline Tablets</i>	Buffer solution
<i>Baird Parker Agar</i>	Culture Medium for <i>S. aureus</i> Assays
<i>Coliform Chromoselect Agar</i>	Culture Medium for <i>E. coli</i> Assays
<i>Cetrimide Agar</i>	Culture Medium for <i>P. aeruginosa</i> Assays

Figure 12. Table of the different media necessary to be able to carry out the bacterial culture for the antimicrobial and antibiofilm tests.

## 4. Methodology

### 4.1. Nanoparticles synthesis

20, 40, and 60 mg of CSA-131 were dissolved in 1 ml of DMSO and mixed with 14:15 ml of 2mg/ml Lauryl Gallate solution, prepared in 96% ethanol. Then, 15 ml, of 1% (v/v) of Tween 80 solution was added to the CSA-131/LG solution while the mixture was subjected to sonication at room temperature for 6 minutes with a 35% amplitude. The resulting NPs were centrifuged for 10 minutes at 1500 rpm using Amicon® centrifugal filters (100 kDa cut-off, Millipore, Madrid, Spain). It is important to note that NPs without CSA-131 were prepared and used as a negative control (non-antibacterial) in all the experiments.

#### 4.1.1. NPs Characterization.

NPs were characterized in terms of their macroscopic appearance, for example, the absence of aggregates and precipitates. The NPs' surface charge, size, and polydispersity were determined using a Zetasizer Nano ZS (Malvern Instruments Inc., Malvern, Worcestershire, UK). The size and the morphology of the NCs were also studied using Scanning Electron Microscopy, SEM (Tecnai G2 F20, FEI Company, Hillsboro, OR, USA), at 80 kV acceleration voltage. Prior to observation, 10 µL of the samples were placed on ultrathin carbon on holey carbon grids and air dried.

#### 4.1.2. Quantification of Total Phenolic Content (TPC).

The total phenol content of the prepared NPs was determined according to the Folin-Ciocalteu method, using gallic acid as a reference. For the assay, different dilutions (4 dilutions 1:10) of the NPs were prepared in mQ water. Then, 20 µl of the NPs were mixed with 100 µl of 20% (w/v) of Sodium Carbonate and 80 µl of 0,2 N Folin-Ciocalteu reagent. The samples were incubated at room temperature and in the dark for 10 minutes. Then, the absorbance was measured at 765 nm using a microplate reader Infinite M200 (Tecan, Austria). Each sample was done in triplicate [13].

#### 4.1.3. Determination of CSA-131 concentration in the NPs.

To start with, a calibration line of 12 standard solutions (1:10) of 0.28 mg/ml of CSA-131 is prepared and dissolved in DMSO in a volume of 75 µL per sample. Afterward, 25µL of 3mg/ml fluorescamine is added as a reagent.

The same volume protocol is used for all samples but in 4 1:2 dilutions from the initial sample which is diluted in 10:100µL of miliQ. water as well as for the negative control of DMSO.

Each of the samples of the three parts must be triplicated [14].

This assay is performed on a black 96-well plate in order to avoid background interference and keep the containing reagents in the dark. One way to do so is by wrapping the container with aluminum foil, to avoid photobleaching. Then, incubate the plate for 3 minutes at room temperature and measure the fluorescence at 390/470nm.

#### 4.1.4. Minimum Inhibitory (MIC) and Bactericidal Concentration (MBC) of the NPs

Prior to the realization of the test, the absorbance of 200  $\mu$ l of overnight grown bacterial suspension in NB was measured spectrophotometrically at  $\lambda = 600$  nm to determine the optical density (OD) and then prepare bacterial inoculum with  $OD_{600} = 0,01 (\sim 10^5 - 10^6 CFU \cdot ml^{-1})$  for the antibacterial tests.

Then, 50  $\mu$ l of the *P. aeruginosa* and *S. aureus* suspensions were mixed with 50  $\mu$ l of the NPs at different concentrations (0.0125–0.2 EO % (v/v)) in a sterile 96-round-bottom-well plate and incubated in at 37 °C for 24 h with shaking. The NB and bacteria served as a negative control (bacterial growth). The absorbance was measured at 600 nm before and after 24 h of incubation. The lowest concentration required to inhibit bacterial growth ( $OD \sim 0$ ) was defined as the MIC. Each sample was tested in a triplicate. The MBC was determined by plating 10 $\mu$ l of each sample and the negative control on selective agar:

#### 4.1.5. Metabolic Activity of bacteria in presence of the NPs

Resazurin assay was performed to assess any changes in the cell's viability induced by the developed NPs. The resazurin assay protocol is based on the reduction of oxidized non-fluorescent blue resazurin to a pink, fluorescent dye (resorufin) by the mitochondrial respiratory chain found in live bacterial cells. The amount of resorufin produced is directly proportional to the number of living cells. For the viability tests, bacteria were incubated with different concentrations of the NPs described before (*Section 4.1 of the Methodology*). After 24 h of incubation, 10  $\mu$ l of 100 mg/ml of resazurin solution was added and incubated for in a dark for 10 minutes at 37 °C. Then the fluorescence was measured at  $\lambda_{(ex/em)} = 520/590$ nm to evaluate bacterial viability [5].

#### 4.1.6. Antibiofilm activity of the NPs: Cristal Violet Assay

The extent of biofilm formation in the presence and absence of the antibacterial NPs was evaluated using a crystal violet assay. Bacterial inoculum was prepared in tryptic soy broth and incubated with the NPs for 24 h at 37 °C in a 96 well plate to allow the biofilm formation. Afterward, the broth was aspirated, and the biofilm was washed three times with 100  $\mu$ l of 100 mM phosphate buffered saline (PBS), at pH 7.2 to remove the non-adherent cells and fixed to the well for 1 h at 55 °C. Then, 100 $\mu$ l of



0,1% (w/v) of crystal violet solution was added for 15 min to stain the biofilm on the plate surface. The excess staining solution was removed by three gentle washes with water, and finally, 125  $\mu$ l of 30 % (v/v) acetic acid was added to each well in order to solubilize the crystal violet bound to the biofilm cells and extracellular matrix. After 10 minutes, the absorbance was measured at  $\lambda = 490$  nm. The amount of crystal violet staining in the assay is directly proportional to the biomass that is attached to the plate [15].

#### 4.1.7. Antioxidant Capacity

The antioxidant activity, as proof for the presence of free phenolic groups on the NPs surface, was determined based on their scavenging activity over ROS using 1 diphenyl-2-picryl hydrazyl (DPPH) free radical in a methanol solution. A total of 0.1 ml of the sample solution was added to 3.9 mL of 60  $\mu$ M of the DPPH free radical solution. After 1 h in the dark, the absorbance of the preparations was measured at 517 nm ( $Abs_{517}$ ) and then, compared to the corresponding absorbance of the blank (DPPH without the sample). Ascorbic acid at 0.5 mg mL<sup>-1</sup> was used as a positive control. The % of inhibition was calculated as follows:

$$\text{Radical scavenging activity (\%)} = ((Abs_{517 \text{ blank}} - Abs_{517 \text{ scavenging activity sample}}) / (Abs_{517 \text{ blank}})) \times 100$$

## 4.2. Sono-enzymatic coating of silicone catheters

### 4.2.1. Silicone Coating with antibacterial NPs by Sono-enzymatic Approach

Polydimethylsiloxane (PDMS) stripes prepared from the same material as the urinary catheters were initially used to allow a proper characterization of the coating otherwise hampered by the curved surface of the catheters. Pieces of 1 x 1 cm<sup>2</sup> were cut and washed in 0.5% (w/v) SDS solution in deionized water for 30 min with constant stirring. After they were washed with deionized water and 96% ethanol, the PDMS stripes were plasma-treated in a radiofrequency reactor operating at 13.56 MHz using O<sub>2</sub> as plasma gas along with a constant flow rate of 15 sccm to generate hydroxyl groups on the PDMS surface at an incident power of 100 W for 5 min. Immediately after plasma treatment, samples were transferred to 100 ml of 5% (v/v) APTES in 96% ethanol for 24 h at room temperature. The samples were finally washed with ethanol to remove the unbound APTES molecules.

10 pieces of APTES-treated PDMS samples (1x1 cm<sup>2</sup>) were placed in a glass vessel containing 18 mL 0,3M Sodium Acetate buffer, pH 5, 9 mL of the CGNPs, 0,838 g of SBMA, and 3 ml of laccase. The coating process was performed in a single step using a high-intensity ultrasound field for 1 h at 50°C and 35% of amplitude. Control samples with only CGNPs were prepared. After the coating process, silicone pieces were washed with miliQ water and subjected to further analysis.

#### 4.2.2. Surface characterisation

Attenuated Total Reflectance–Fourier Transformed Infrared (ATR–FTIR) spectra of pristine and modified silicone samples over the 500–4000  $\text{cm}^{-1}$  range were collected by a PerkinElmer Spectrum 100 FTIR spectrometer, performing 100 scans for each spectrum at a 4  $\text{cm}^{-1}$  resolution. Fourier Transform Infrared Spectroscopy (FTIR) is an analytical tool that uses infrared radiation to excite molecular movements that subsequently are recorded. Every functional group has its wavelengths from within the spectrum that causes a specific vibration, like activation energy [2].

#### 4.2.3. Determination of the hydrophilic property

Sulfobetaines are zwitterions that possess antifouling properties due to their capacity to bind water molecules and create a barrier for different compounds to adhere to the surface. The contact angle of the differently treated samples was measured with a Drop-Shape analyzer DSA 25 (Krüss, Germany). Briefly, the measurements were performed at room temperature in the air by applying the sessile drop method. Liquid drops of 2  $\mu\text{l}$  were applied to the material surface. The contact angle measurements for the determination of the hydrophilic/hydrophobic characteristics were estimated by the two-dimensional projection of the droplet, on both left and right sides.

#### 4.2.4. Protein Adsorption

Silicone samples (1 cm  $\times$  1 cm) were immersed in a 1 mg  $\text{ml}^{-1}$  albumin-fluorescein isothiocyanate conjugate (FITC–BSA) solution (w/v) for 30 min to simulate the immediate process of protein attachment preceding the biofilm formation. [6] After that, the samples were rinsed with deionized water and dried with nitrogen. The protein attachment on the pristine and coated silicone surfaces was evaluated using a fluorescence microscope NIKON Eclipse Ti-S (Nikon Instruments, Inc., Amstelveen, The Netherlands).

#### 4.2.5. Antimicrobial activity of NP coated silicone

The antibacterial activity of the functionalized silicone materials was assessed against Gram-negative *P. aeruginosa* and Gram-positive *S. aureus*. To sum it up, single colonies of bacteria were grown in Mueller Hinton Broth at 37 °C and 230 rpm overnight. Then, the bacteria were diluted in 100 mM phosphate-buffered saline (PBS, pH 6.8) (colony forming units (CFU)  $\text{mL}^{-1} \sim 10^8$ ); subsequently, 1 piece (1  $\times$  1  $\text{cm}^2$ ) of silicone was placed with 1.5 ml of bacteria in 15 ml sterile falcons and incubated for 24 h at 37 °C and 230 rpm shaking. The bacterial withdrawn suspensions were serially diluted in sterile 100 mM PBS, plated on selective Cetrimide and Braid Parker agars, respectively, and incubated for 24 h at 37 °C, and the viable bacteria were counted using the drop count method.

#### 4.2.6. Antibiofilm activity

As previously described, the ability of the developed coatings to impede the biofilm formation on the modified silicone materials was assessed with *P. aeruginosa* [14]. Briefly,  $1 \times 1 \text{ cm}^2$  of silicone was incubated with 1.5 ml of bacterium ( $\text{OD}_{600} = 0.01$ ) in tryptic soy broth (TSB) in a 24-well microplate. The microplate was incubated for 24 h at  $37^\circ\text{C}$  under static conditions, allowing the bacteria to colonize the silicone materials and therefore form biofilms. Following the incubation, the nonadherent bacterial cells were washed three times with 2 ml of sterile 100 mM PBS (pH 6.8), and the bacterial biofilms were fixed for 60 min at  $60^\circ\text{C}$  and stained with 1 ml of 0.1% (w/v) crystal violet solution for 15 min. Subsequently, the silicone pieces were placed with 1 ml of 30% acetic acid (v/v) to redissolve the crystal violet dye fixed on the samples. The absorbance of the resulting solutions was measured at 595 nm.

#### 4.2.7. Live/Dead Kit Assay

The live and dead bacteria in the biofilms formed on the silicones were also assessed using Live/Dead BacLight Kit assay. After the biofilm development, the samples obtained were stained with a mixture of Syto 9 and Propidium iodide (PI) (1:1) for 15 min. The biofilms were rinsed with  $100 \mu\text{l}$  of 100 mM PBS (pH 6.8). Moreover, the samples were analyzed by fluorescent microscopy at Ex/Em 480/500 for Syto 9 staining the live bacteria and PI at Ex/Em 490/635 labeling the dead bacteria. The stained biofilms were observed under  $20\times$  magnification. The live cells were stained in green and the dead ones in red.

Fluorescence microscopy at Ex/Em (480/500) for Syto<sup>®</sup> 9 labeling the nucleic acid of all bacteria, with intact and damaged membranes in green and at Ex/Em (490/635) for propidium iodide quenching the green fluorescence of Syto<sup>®</sup> 9 dye after penetration into the damaged cells, consequently staining dead bacteria in red.

## 5. Results and Discussion

### 5.1. Nanoparticles Characterisation

#### 5.1.1. DLS and Z potential

Table 1 determines the size and zeta-potential of sonochemically prepared CGNPs using 20, 40, and 60 mg/mL of CSA in the reaction. Empty NPs had a zeta potential of  $-28,83 \pm 1,06$  mV while loaded CSA nanovesicles showcased positive surface charge varying from 22 to 30 mV -depending on the initial amount of CSA in the reaction mixture-. The change in the surface charge of empty lauryl gallate NPs is most likely due to the presence of positively charged ceragenin molecules in the in NPs shell. As for the hydrodynamic size of the NPs, CGNP demonstrated a larger size than the control empty LG NPs.

Considering this analysis, CGNP of 40mg/ml has been chosen for its polarity and stability index. Moreover, its physicochemical properties are suitable for a better coating of silicones, as there is greater interaction with the environment.

NP sample	CSA [mg/ml]	Zeta-potential (mV)	Size (d.nm)	Pdl
NP	-	$-28,83 \pm 1,06$	$1352 \pm 38,18$	$0,96 \pm 0,05$
CGNP	20	$29,43 \pm 0,47$	$740,67 \pm 13,84$	$0,57 \pm 0,04$
CGNP	40	$25,23 \pm 0,32$	$1295,50 \pm 214,25$	$1,00 \pm 0,00$
CGNP	60	$22,6 \pm 1,31$	$941,65 \pm 64,84$	$0,77 \pm 0,05$

Figure 13 Table of the values obtained from the DLS and the Z Potential, for each of the CGNP variants using

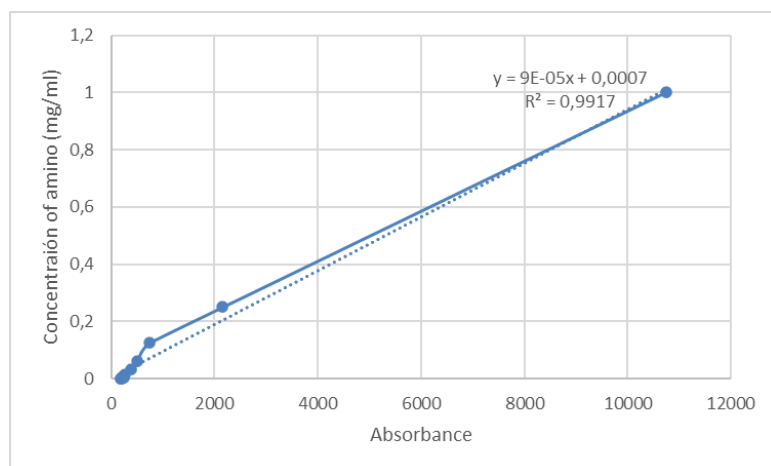
#### 5.1.2. CSA Quantification

Fluorescamine assay for CSA quantification was carried out with CGNP prepared using 40 mg/ml of CSA-131. This test reflects the previous hypothesis since the number of phenols of the CGNP is lower than for the empty NPs at the same concentration, indicating ceragenin presence at the surface.

Data pre-processing was performed with negative control subtracted from the average of each sample to reduce the influence of the DMSO signal and obtain the amino group content.

Pre-processing data was combined with negative control subtracted from the average of each sample in order to reduce the influence of the DMSO signal in order to obtain the amino group content.

A calibration curve was made with gallic acid as a standard to calculate the concentration of primary amines present in each sample (Figure 14).



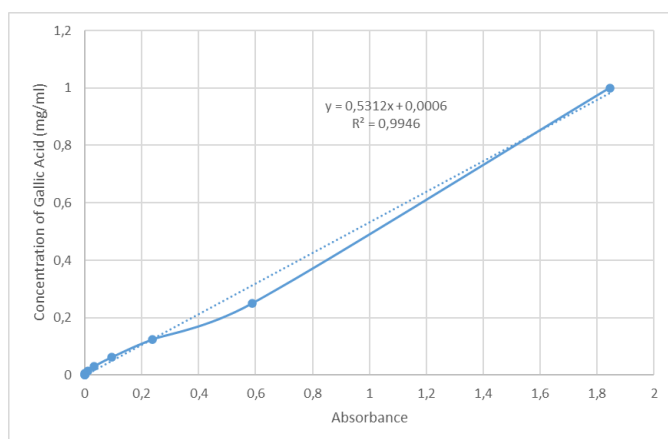
CGNP (mg/ml)	Absorbance
1,00E+00	22255,00
1,00E-01	12698,50
1,00E-02	7277,00
1,00E-03	3983,50
1,00E-04	174,33

NP (mg/ml)	Absorbance
1,00E+00	211,50
1,00E-01	200,50
1,00E-02	197,50
1,00E-03	189,00
1,00E-04	177,00

Figure 14 Calibration curve built using DMSO as a standard and the absorbance values obtained for different concentrations of CGNPs. Samples were prepared with 40 mg/mL initial CSA-131. Concentration was only analysed.

### 5.1.3. Quantification of Total Phenolic Content (TPC)

A total phenolic content assay was carried out with CGNP prepared 40 mg/ml of CSA-131. Then, the total amount of phenols was calculated through a linear equation (Figure 15), based on the calibration curve from the absorbance of the standard sample (gallic acid).



CGNP (mg/ml)	Absorbance
1,00	1,60
0,10	0,25
0,01	0,03

NP (mg/ml)	Absorbance
1,00	1,78
0,10	0,28
0,01	0,03

Figure 15. Calibration curve built using gallic acid as a standard and the absorbance values obtained for different concentrations of CGNPs. Samples were prepared with 40 mg/mL initial CSA-131. Concentration was only analysed.

#### 5.1.4. Scanning Electron Microscope

The size and morphology of the developed CGNP were studied using a *PhenomXL*. The SEM obtained a clear image of spherical in shape nano-sized entities with an average size of 500 – 700 nm separated from each other. The lack of agglomerates indicated colloidal stability as it is in agreement with the zeta-potential measurements.

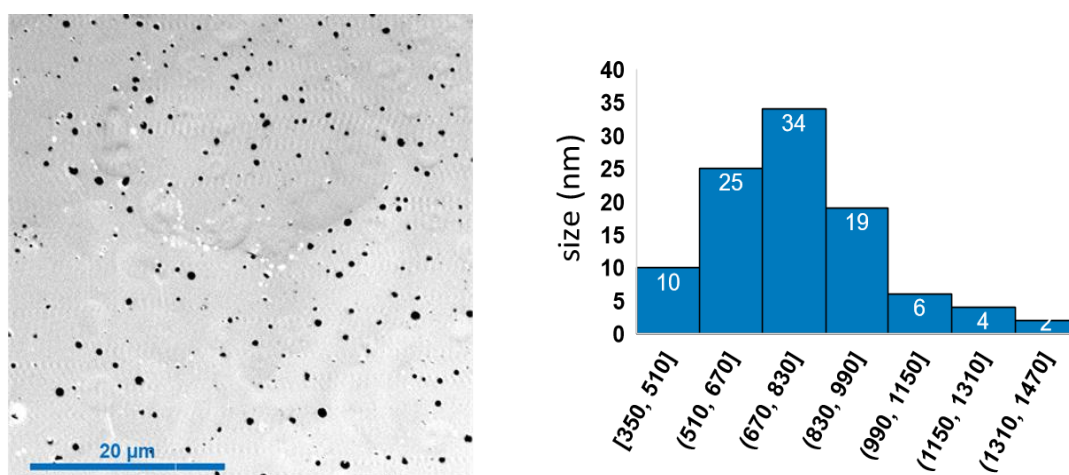


Figure 16. SEM images of CGNPs (left). Histogram of CG NPs size distribution based on the total count using ImageJ software (right).

#### 5.1.5. Antioxidant activity

The assay was carried out with the same concentration found in the Determination of Phenol Content (Section 5.1.2. of Results and Discussion), through the relationship between the functional group and the antioxidant capacity. Data pre-processing was performed with negative control subtracted from the average of each sample to sweep the medium signal and therefore obtain the resulting absorbance for each test.

The results are the absorbance of unoxidized free radicals, meaning that the remaining percentage part was plotted (Figure 17). For this, the positive control has been considered as the maximum percentage. The measurement error of each triplicate sample has also been calculated.

The oxidative capacity of both particles is high, which indicates that the exposed bacteria to their oxidative stress lose the ability to defend themselves against free radicals, unbalancing their cell membrane while increasing their susceptibility by not being able to stimulate antioxidant preventive and repair agents -such as catalases and superoxide dismutases.

At small concentrations, a slightly higher effectiveness is observed in NPs than in CGNPs. This result is directly related to the slight difference obtained in the phenol content of the Determination of Phenol Content test (Section 5.1.2. of Results and Discussion).

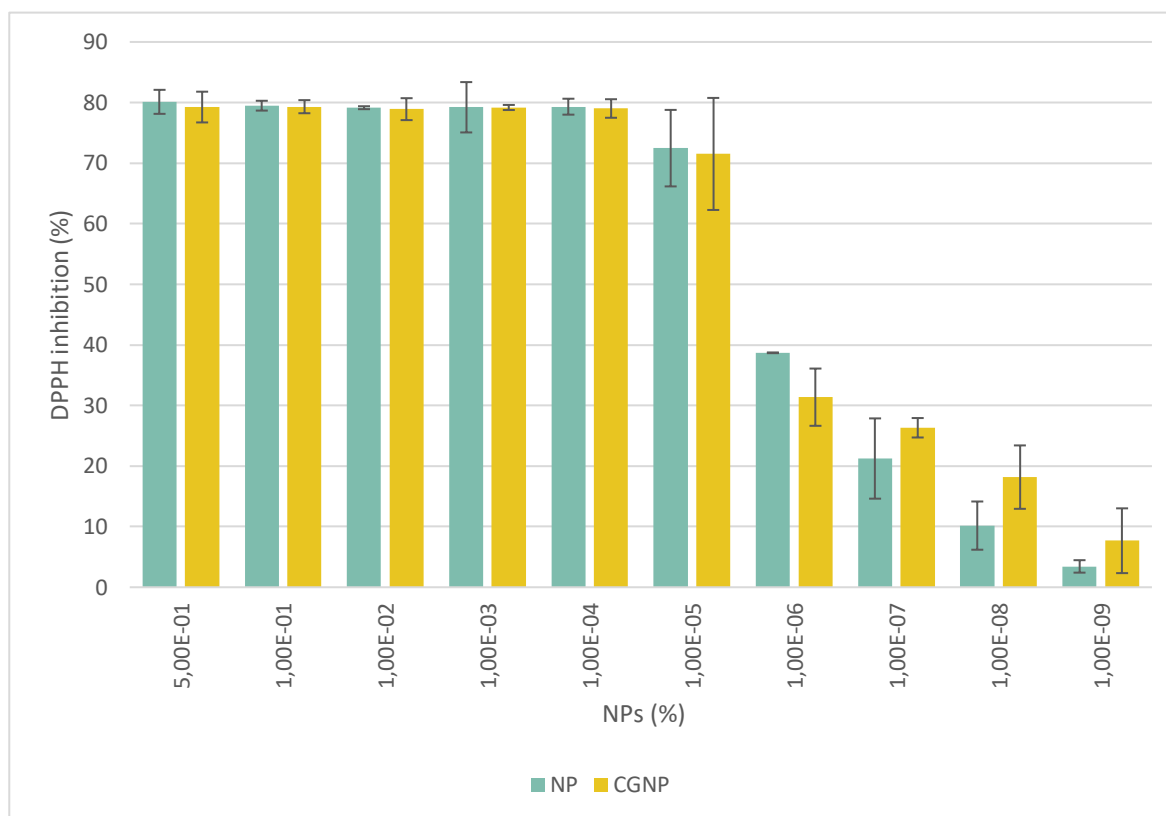
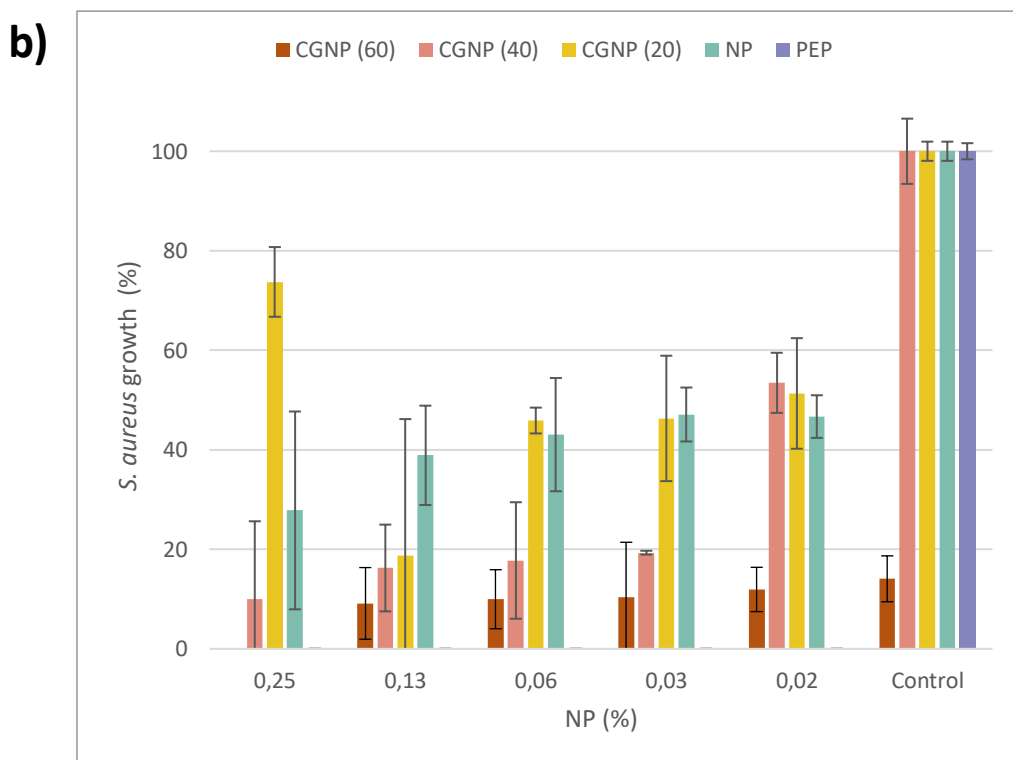
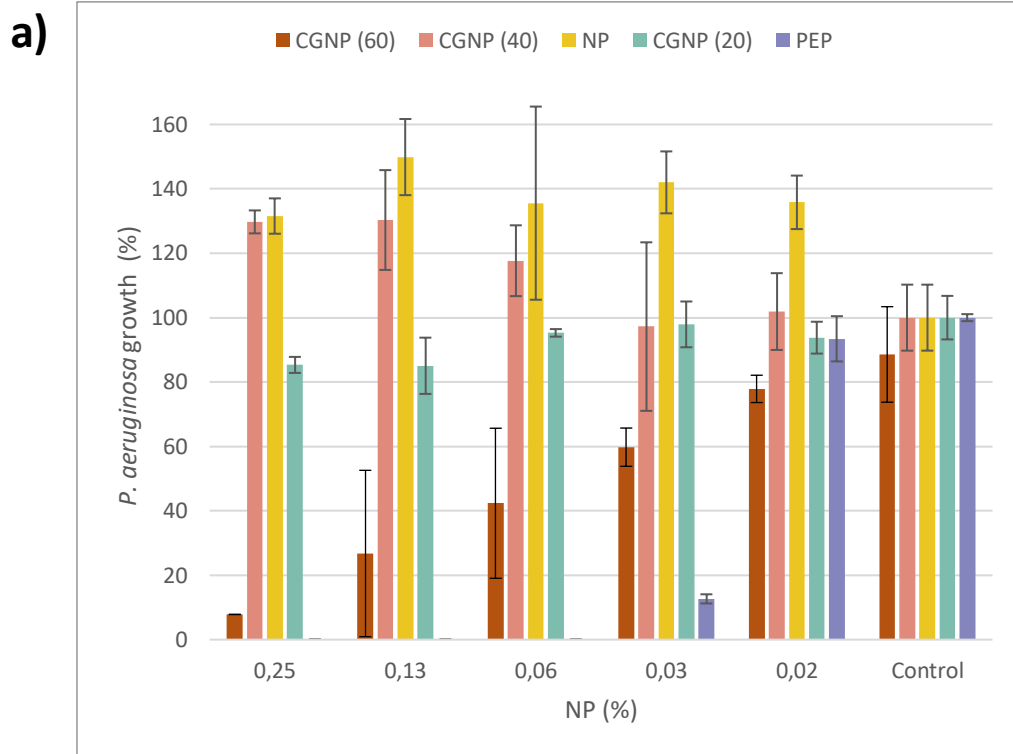


Figure 17. Representation of the antioxidant activity of CGNPs and NPs. Its reducing capacity does not decrease until dilution 1:1,000,000.

### 5.1.6. Antimicrobial activity of the nanoparticle properties

The minimal inhibitory concentration (MIC) of the CGNPs prepared to employ 20, 40, or 60 mg/mL bulk CSA-131 in the reaction process is determined against *P. aeruginosa*, *S. aureus* and *E. coli* by a standard broth dilution method. Data pre-processing was performed along with a negative control (only MHB) subtracted from the average of each sample in order to eliminate the influence of the medium signal and obtain the resulting absorbance. Consequently, the percentage of each bacterium growth was determined by the difference in the absorbance at the beginning of the experiment (t<sub>0</sub>) and after 24 h of incubation (t<sub>24</sub>) with respect to the positive control –bacterium without antibacterial activity-. The results were carried out from the 1:4 dilution due to the high effectiveness in higher concentrations. The measurement error of each triplicate sample has also been calculated.





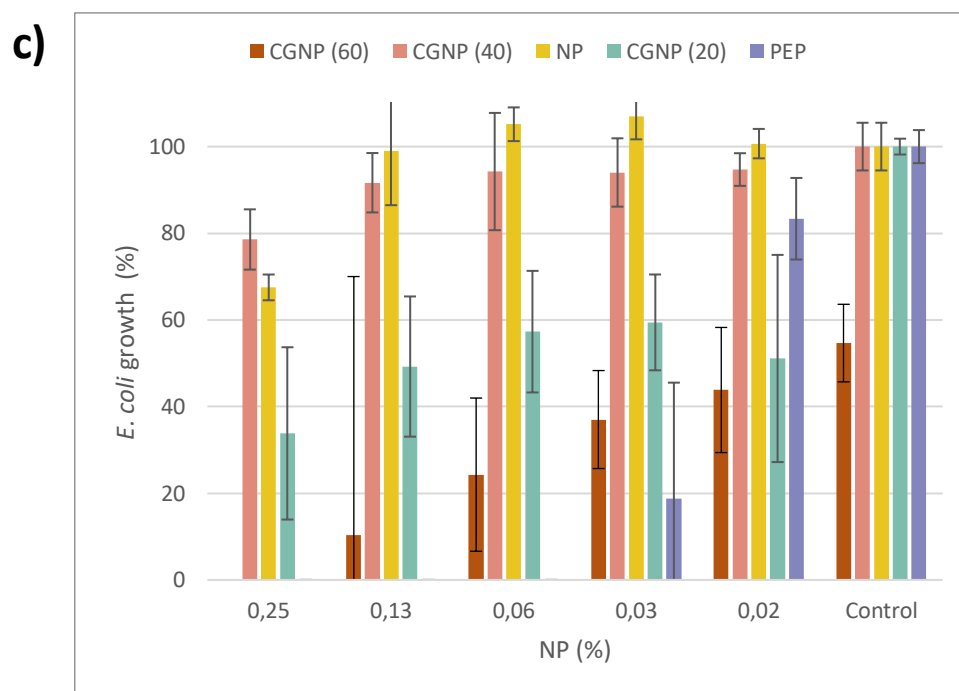


Figure 18. A) *P. aeruginosa*, B) *S. aureus* and C) *E. coli* growth (%) after 24 h incubation with CG NPs at different concentrations.

Regarding the MBC, the generated colonies from each bacterium in its agar were counted to represent the bactericidal effect of the nanoparticles. (Figure 19)

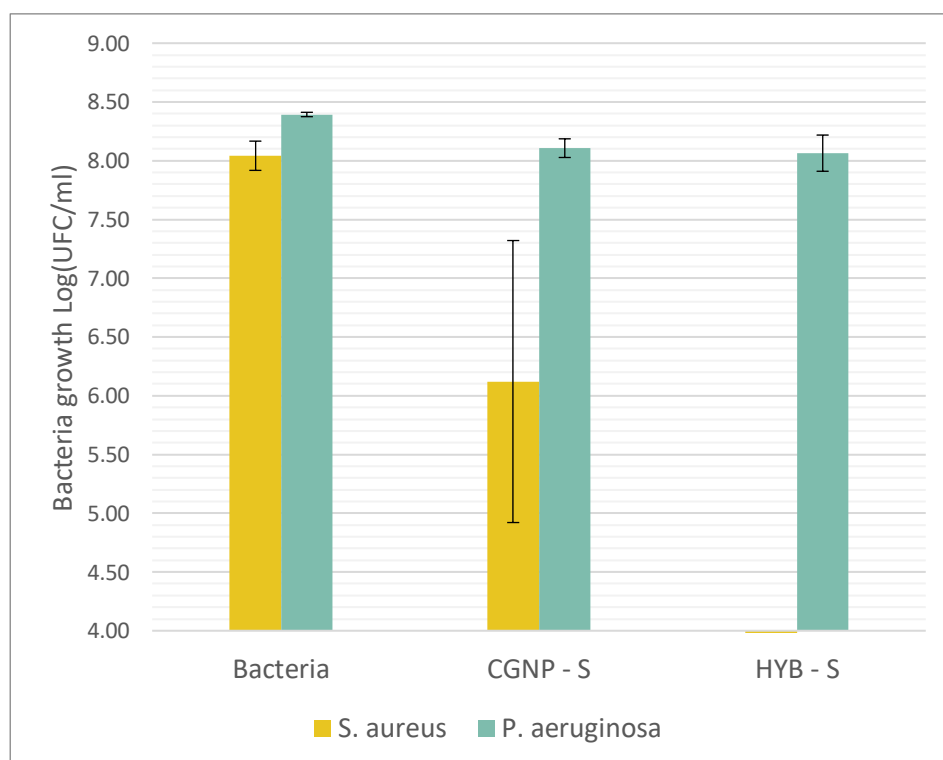


Figure 19. *S. aureus* and *P. aeruginosa* growth (%) after 24h h incubation with CG NPs

After several tests, it was confirmed that the developed CGNPs possess a higher antimicrobial effect on *S. aureus* and *P. aeruginosa*, while their use in inhibiting the growth of *E. coli* is not of interest, due to the lower effect on this bacterium (Figure Z). Gram-negative bacteria are more resistant because of their cell wall used as protection.

The concentration of 40 mg/ml has been considered to be optimal for the CGNPs development since a higher amount of CSA-131 in the synthesis reaction (60 mg/mL) did not result in the improvement of the NPs bactericidal effect. Moreover, 40 mg/mL led to the formation of stable NPs with strong bactericidal effects. It is noteworthy to mention, that the concentration of 60 mg/ml has been discarded due to the miscibility problems found during the process, which would later on explain the analyzed results. The concentration of 20 mg/ml has also been discarded due to the low stability and antimicrobial efficiency (Figure X). It has been observed that many of the absorbances exceed the positive control when this is considered the maximum growth in the absence of any surrounding bactericide. This factor leads to the establishment of the hypothesis that the NP-suspended gives signals.

For this reason, MBC is performed to quantify colony growth. The CGNP of 40mg/ml concentration was chosen. The MIC results highlighted that the CGNP showed exposure signals of *S. aureus*. However, nothing has grown on the MBC test. Therefore, the hypothesis is considered to be correct. Finally, it is considered that the best concentration is the CGNP of 40mg/mL, but, since the results are not very fruitful, a study of the effect of CGNP on the metabolism of *S. aureus* and *P. aeruginosa* bacteria is considered (Section 1.1.3 of Results).

### 5.1.7. Metabolic Activity of Bacteria

The purpose of this test was to confirm the killing potential of the developed NPs with the intention to clarify the MIC and MBC results. The metabolic assay revealed that the combination of Lauryl Gallate and CSA-131 possesses a greater effect on metabolism compared to the empty NPs (Figure X), in all three bacteria studied. Consequently, CSA-131 has effects on the metabolism. The aforementioned results demonstrate that the peptide alone (PEP) also has a bactericidal and bacteriostatic effect (Figure). CGNPs are considered to give a signal in the MIC assay as the release of ceragenins is slow. First, as NPs do, they generate a ROS effect against the bacteria. However, as demonstrated by the assay, NPs do not have the antibacterial capacity (Figure 20).

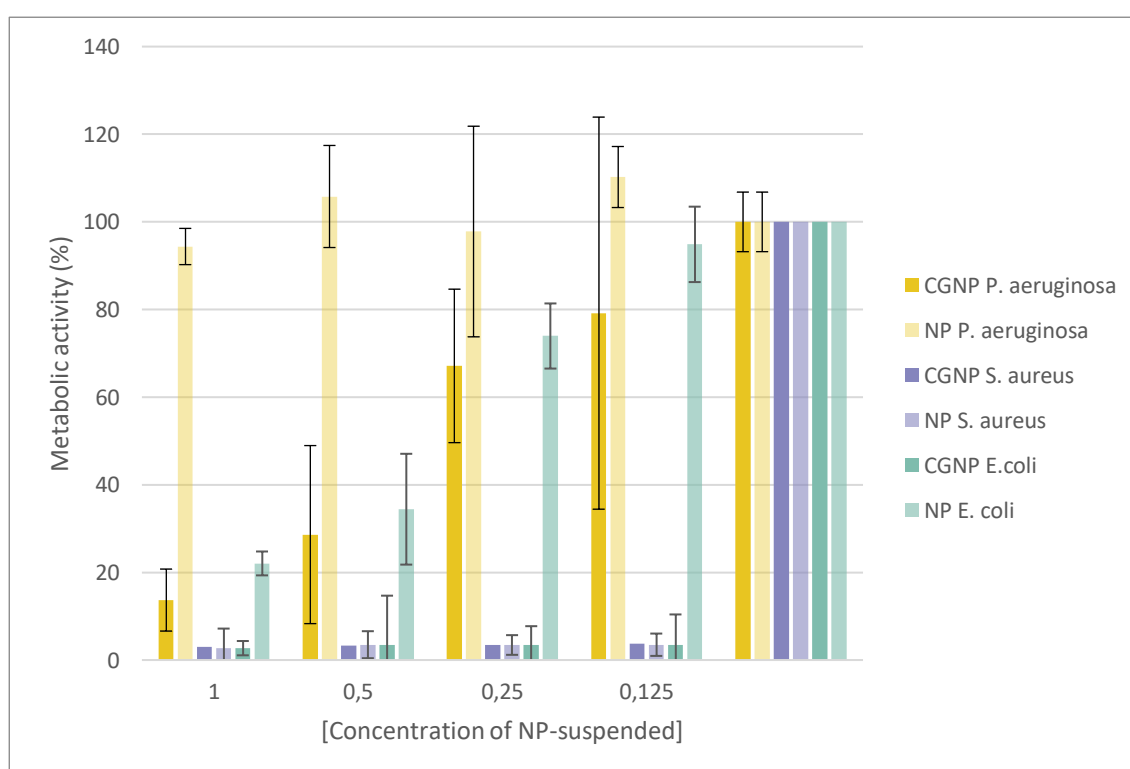


Figure 20. Representation of the effect of CGNP and NP on the metabolism of Grampositive and Gramnegative bacteria

### 5.1.8. Antibiofilm Activity of CGNPs

Pre-processing data was performed with negative control subtracted from the average of each sample in order to sweep the medium signal and obtain the resulting absorbance for each test.

Due to the high effectiveness in higher concentrations, the study was carried out with a 1:4 dilution of the NPs. The results obtained were plotted to represent the percentage of bacterial biofilm

formation (Figure 21). For this, the absorbance of the positive control has been considered as maximum growth. The measurement error of each triplicate sample has also been calculated.

Considering that only a saturated signal was obtained, the *P. aeruginosa* bacteria could not be plotted. Nonetheless, it can be observed that the CGNP does have antibiofilm capacity. For that reason, sulfobetaine is used in the coating to help prevent the formation of biofilm while the nanoparticles fulfil their bactericidal capacity.

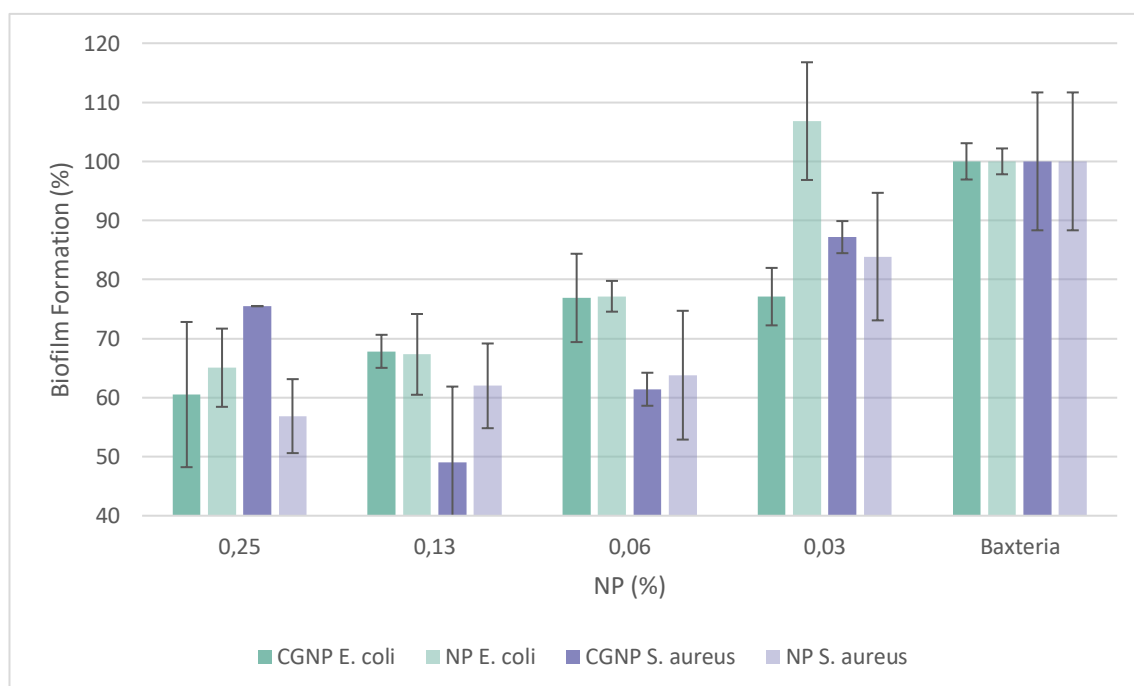


Figure 21. *E. coli* and *S. aureus* biofilm growth (%) after 24h h incubation with CG NPs

## 5.2. Sono-enzymatically Enzymatically Triggered Bottom-Up functionalization of silicones

Antimicrobial and antifouling nano-enabled coating were constructed on urinary catheters in a sono-enzymatically triggered bottom-up approach. At first, silicone material was plasma-activated and pre-nominated with (3-aminopropyl)triethoxysilane (APTES), allowing subsequent laccase-catalyzed grafting of the CGNPs. Subsequently, the tethered phenolic residues from the CG NPs were activated by laccases to phenoxy radicals, triggering an enzymatically initiated radical polymerization of zwitterionic carboxybetaine methacrylate monomers on the silicone catheters in a “grafting from” process under the US field.

A quadruplicate of the following samples has been used for the following tests:

- Pristine silicone (S)
- Silicone functionalized with APTES (APTES-S)
- CGNPs coated silicone (CGNP-S)
- Silicon coated with a combination of sulfobetaine and CGNPs-suspended (HYB-S)

### 5.2.1. Characterisation of the nano-enabled coating

Fourier Transform Infrared Spectroscopy (FTIR) was used to characterize the chemical groups on the surface.

From the resulting graphs, an amino signal (1534  $\text{cm}^{-1}$ ) can be observed in the APTES-S graph that reflects the plasma treatment of the pretreated silicone. On the other hand, a hydroxyl signal is observed throughout the spectrum (3200-3600  $\text{cm}^{-1}$ ) in the CGNP-S graph that indicates a greater number of interactions and molecular movements resulting a greater dispersion of frequencies, surely from the phenolic groups of Lauryl Gallate. Finally, a slight signal of the sulphate group (1463  $\text{cm}^{-1}$ ) is observed, indicating the existence of sulfobetaine on the surface of the silicone. Its signal is weak when it is attenuated by the amide signal (1650  $\text{cm}^{-1}$ ). This functional group is generated by joining an amine and a phenol, implying a low amine and hydroxyl signal due to an increase in the amine signal due to the combination of sulfobetaine with Lauryl Gallate, just like the CGNP-S graph, due to the union of the APTES with the Lauryl Gallate.

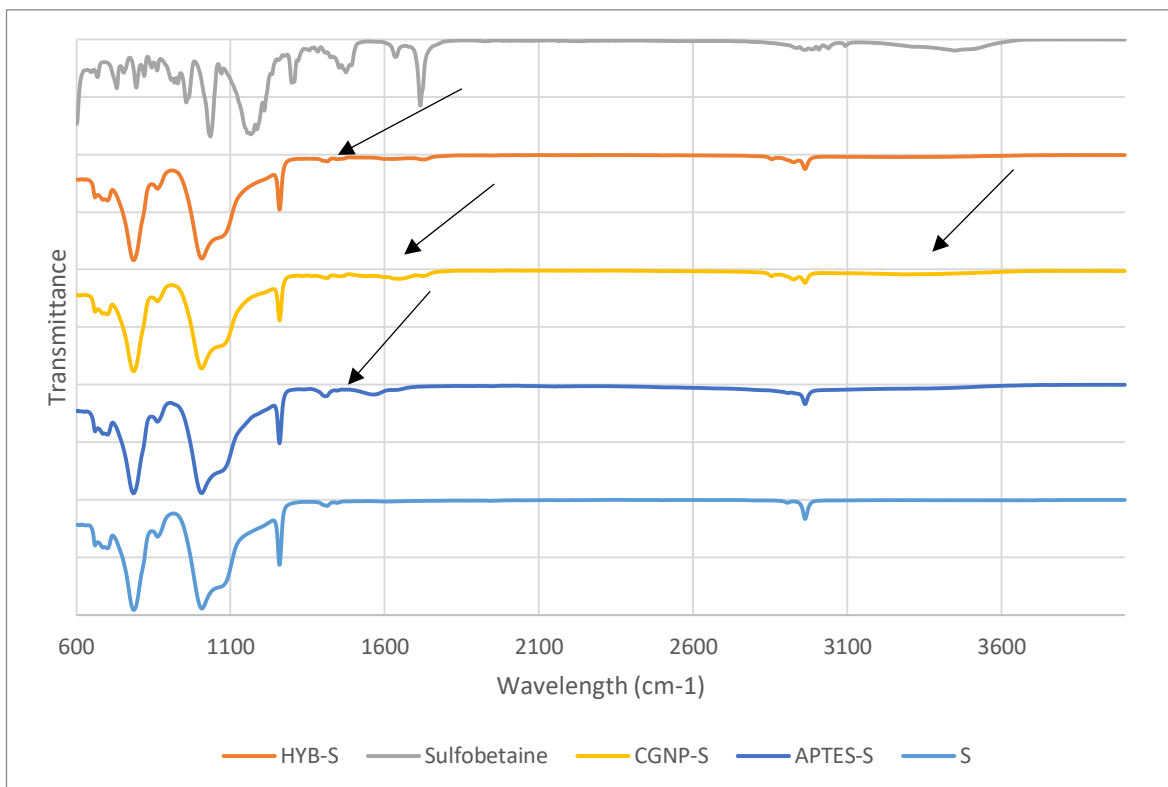


Figure 22. ATR-FTIR spectra of each sample of silicone.

## 5.2.2. Water Contact Angle Measurements

The hydrophilicity -a property required for materials intended to present low organic matter adsorption of the resulting surfaces after the different modification steps- was evaluated with the Static Contact Angle. The results were performed and analyzed for each sample. The contact angle measurements demonstrated that coating samples have more hydrophobicity, which accounts for the measured value for the water contact angle when this is below  $90^\circ$ .

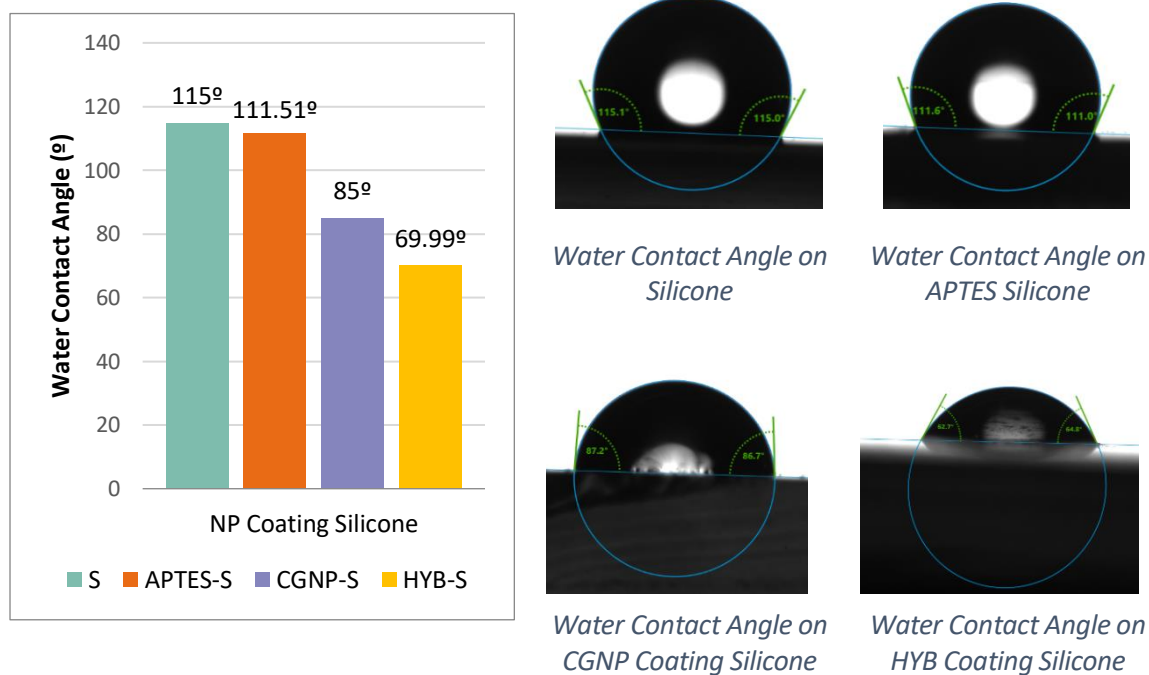


Figure 23. Representation of the silicone hydrophilicity character as it is treated, with photos of the drop reaction once it falls on the surface.

### 5.2.3. Initial Protein Attachment

Proteinuria, or the presence of plasma proteins in urine, is a common condition in patients presenting UTIs. Such proteins are capable of adsorbing onto hydrophobic surfaces, such as silicone, serving as a conditioning layer favoring the attachment of bacteria and subsequent biofilm growth. The protein attachment on the surface of the silicone samples was evaluated using a fluorescence microscope NIKON/Eclipse Ti-S (Nikon Instruments, Inc.).

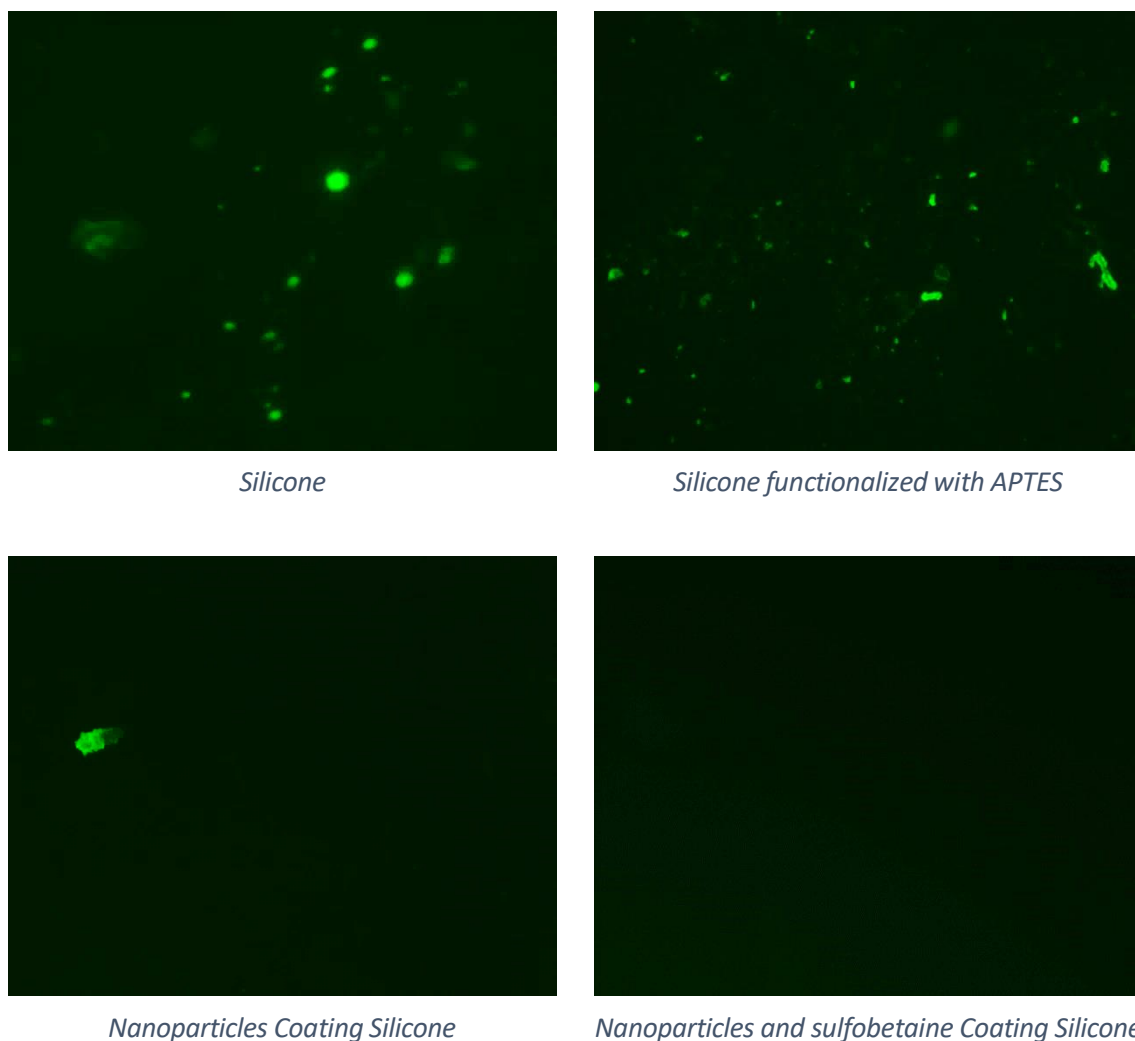


Figure 24. Images taken from the microscope of the qualitative amount of protein adhered to the surface of the different silicones.

A decrease in fluorescence is observed in the order of the images because of the decrease in the adhered protein, thus indicating that the hybrid coating sulfobetaine possesses antifouling properties and will therefore reduce the protein and bacterial attachment on the catheter surface.



### 5.2.4. Antimicrobial activity of nano-enabled silicone

The results obtained indicate a lower bacterial growth in the CGNP-S and HYB-S silicones. Its antimicrobial effect could correspond to the coating of CGNPs made on the surface and thus affirm its bactericidal capacity. In the case of *S. aureus*, no growth is observed, considering that the coating is more highly effective in Gram-positive bacteria than Gram-negative representatives, which shows more resistance and possibly due to the different structure of the cell wall. However, *P. aeruginosa* offers a different response between both silicones, HYB being more effective as it contains sulfobetaine as an antibiofilm agent, hindering the adhesion of bacteria to the surface.

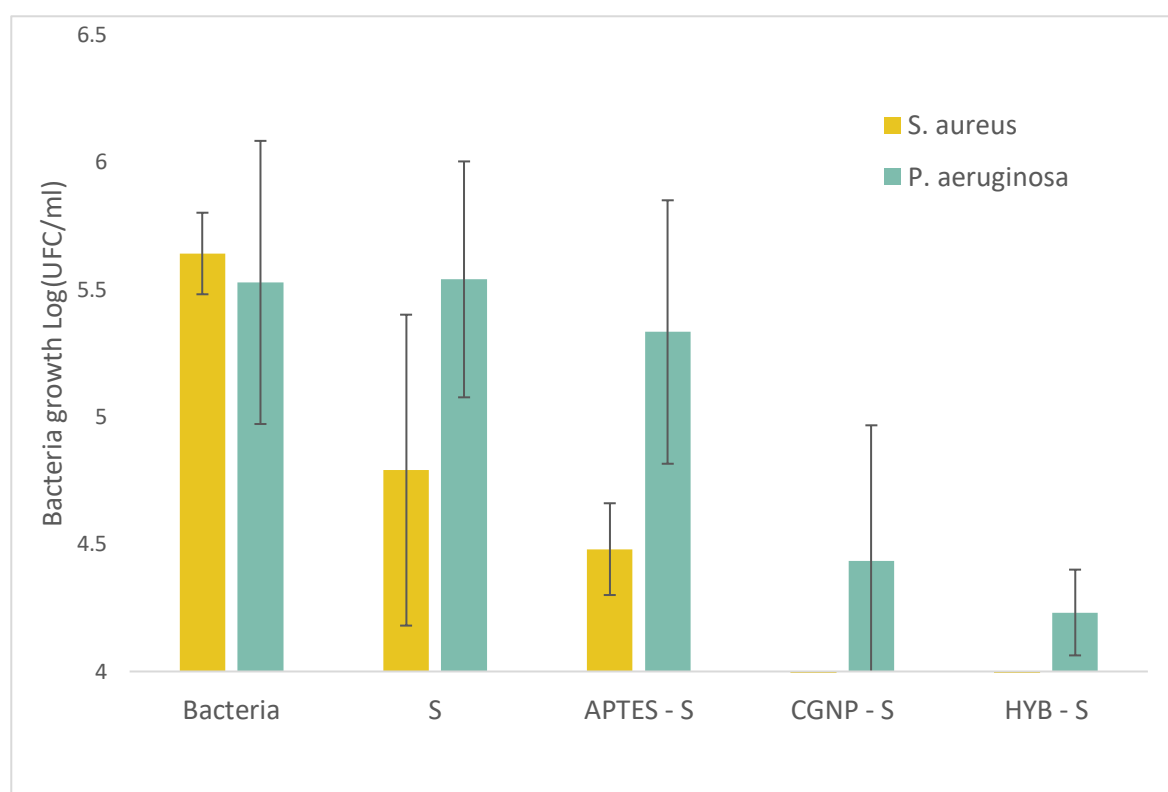
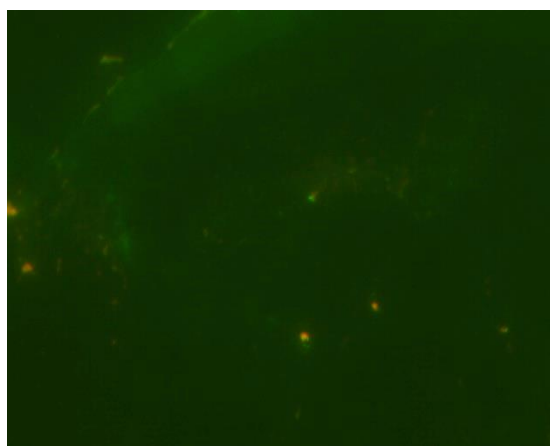


Figure 25. Representation of *P. aeruginosa* and *S. aureus* biofilm growth (%) after 24h incubation with each silicone sample.

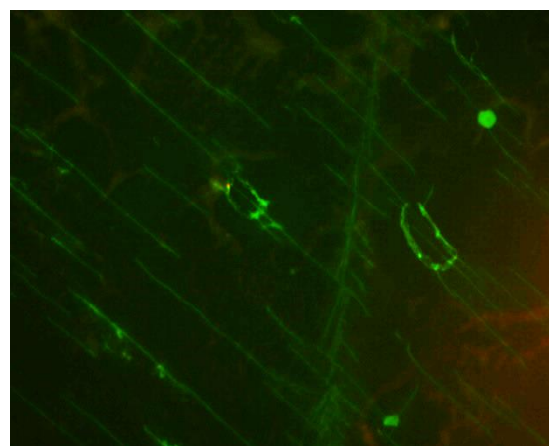
### 5.2.5. Live/Dead Kit Assay

*P. aeruginosa* and *S. aureus* were studied using live/dead assay with fluorescence microscope NIKON/Eclipse Ti-S (Nikon Instruments, Inc.). The information available from these images (Figure 26, 27) corresponds to the data from the antimicrobial tests. The appearance of red cells in the images do not confirm the antimicrobial capacity of CGNP against bacteria because of the poor quality of the images.

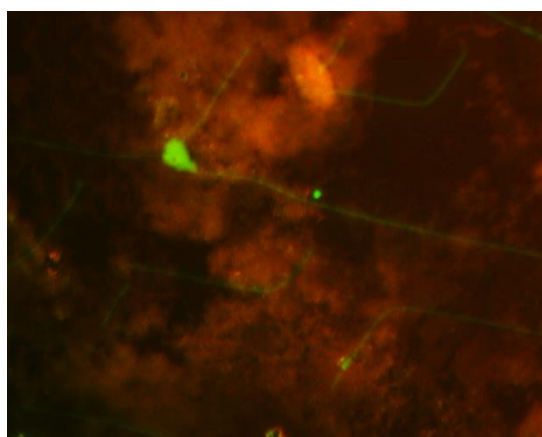
Otherwise NPs hybridization with zwitterions will improve the antibiofilm activity of the silicone, leading to a decrease in bacterial adherence and thus, the complete eradication of the attached cells - stained in red-. The zwitterionic component provides a barrier for the bacteria to adhere to and form an extracellular matrix, protecting them from antimicrobials. Therefore, it makes the individual cells more susceptible to the bactericidal CGNP in the coating, leading to complete bacterial removal and sterilization of the catheter surface.



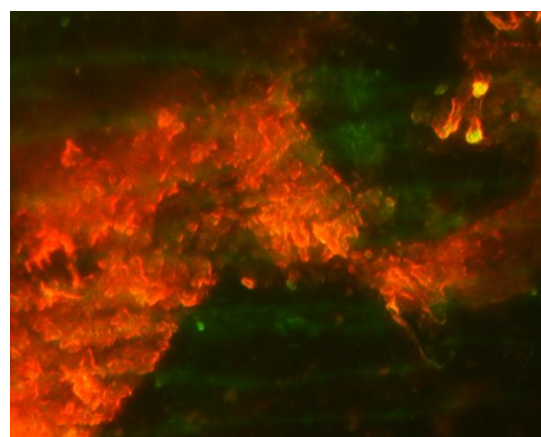
*Silicone*



*Silicone functionalized with APTES*

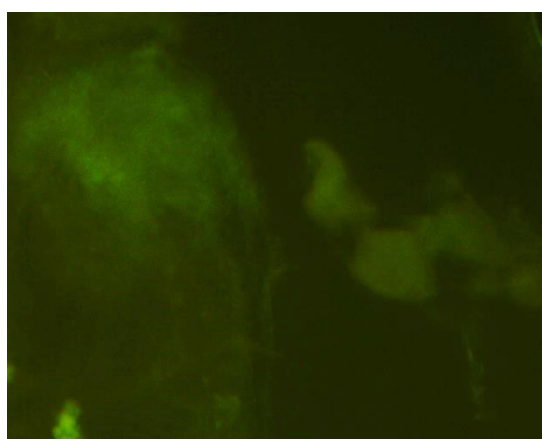


*Nanoparticles Coating Silicone*

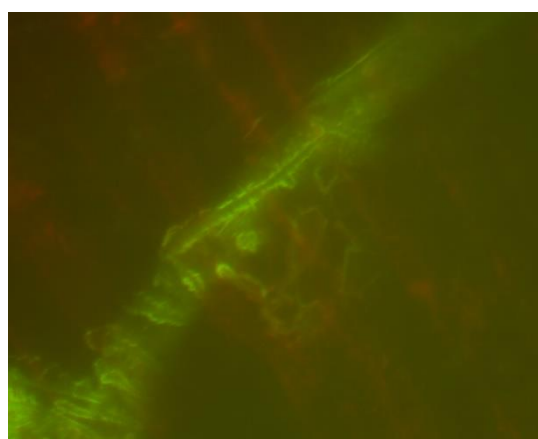


*Nanoparticles and sulfobetaine Coating Silicone*

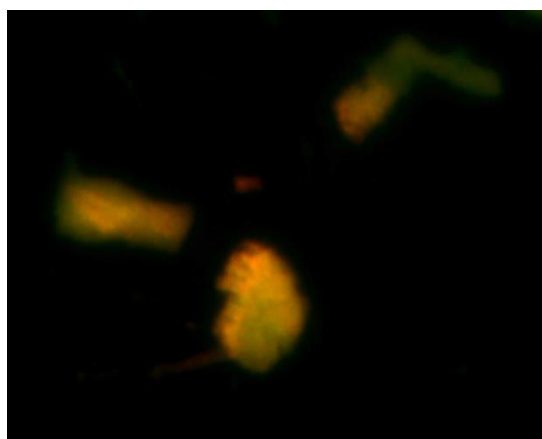
Figure 26. Live/Dead assay images of *S. aureus* cultures in the four types of silicone sample. They are not consistent.



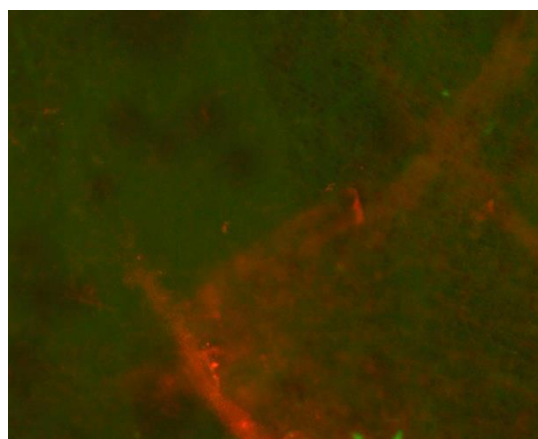
*Silicone*



*Silicone functionalized with APTES*



*Nanoparticles Coating Silicone*



*Nanoparticles and sulfobetaine Coating Silicone*

*Figure 27. Live/Dead assay images of P. aeruginosa cultures in the four types of silicone sample. They are not consistent.*

## 6. Environmental study

This project consists of the preliminary part of the research -carrying its development in the laboratory, meaning that it is not possible to generate a broad analysis of the environmental impact of its production. Consequently, an analysis of the experimental part has considered the components used during the process as well as both the possible impact if not handled correctly and the energy impact regarding the formation of the object of study.

To clarify, an environmental impact is defined as any action that involves the transformation or change in the balance of an ecosystem and, therefore, the well-being of society and the environment.

### 6.1. Environmental Impacts of the Experimental Phase

In order to identify these key points, the following possible causes of each activity have been taken into account:

- The use of contaminants reagents.
- The use of bacteria.

To prevent both cases, it must be avoided the cause of the environmental impact, which could be determined by malpractice in the laboratory. Regarding the different reagents used, laboratory regulations must be applied in reference to the necessary equipment to work. These include a gown, goggles, and gloves to avoid direct contact with the substances. It is important to keep in mind the correct handling of the different components, including how to store them in their respective conditions so that they do not detonate, spill, or spoil. The last important factor is the correct management of the waste produced as a way to avoid contamination of the laboratory and the environment. Therefore, its subsequent treatment is carried out by the contracted company by the laboratory.

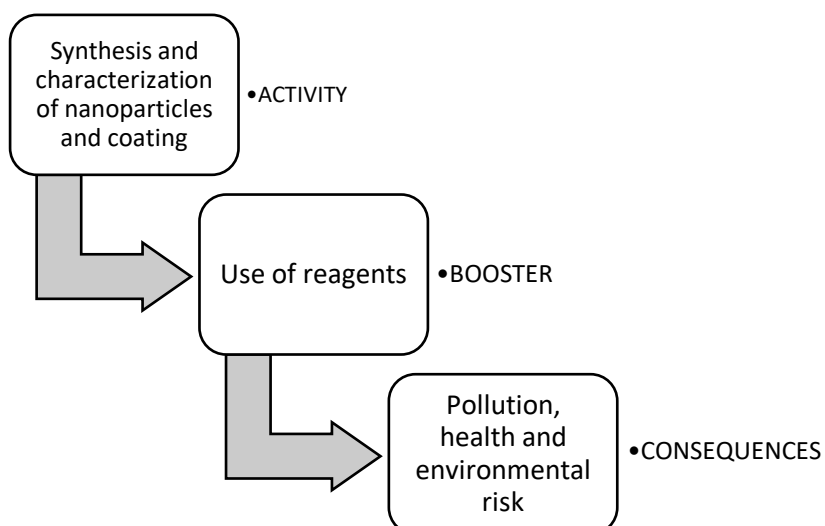


Figure 28. Diagram of three phases of the environmental impact with the misuse of reagents

Referring to the use of microorganisms, it is equally important to use the correct laboratory equipment to avoid exposure to pathogens and, subsequently, spread it on to the rest of the staff. Its handling must be done conscientiously by keeping the workplace disinfected and discharging the cell cultures in a suitable container that hinders bacterial growth.

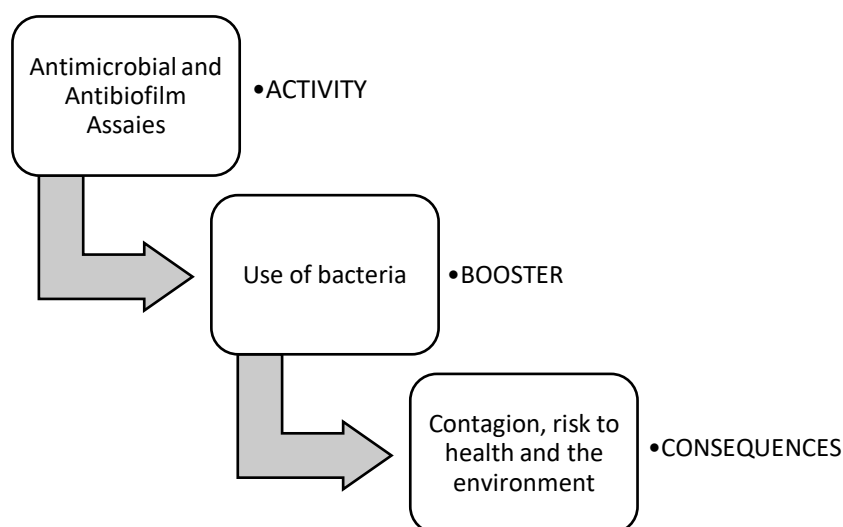


Figure 29. Diagram of three phases of the environmental impact with the misuse of bacteria.

## 6.2. Environmental Impact of Production and Product

To start with, it is important to note that the production scale of this study is not applicable to the industrial scale, meaning that it is not possible to generate an analysis of the impact that can be generated. However, the generated product would not pose a threat to society's health since, due to problems regarding deposition and the elements in the production, it has been designed to be biocompatible and, therefore, unable to generate health problems. Nonetheless, the final results were obtained via in vitro experiments. An in vivo study of ceragenins has not yet been performed.

## 6.3. Environmental Impact Due to Energy Consumption

In order to obtain the results of this project, a number of electrical devices that require electrical energy for their operation have been used. Then, the power required for each element has been calculated and multiplied by the time of its use. Once the final value is obtained it will calculate the carbon dioxide per kW · h consumed, which results in 0.273kg per kW · h [11].

The powers required for each device have been obtained by searching over the elements of *Section 3.2. of Materials*.

Equipment	Potencia (kW · h)	Time (h)	CO2 Consume (Kg)
<i>Vortex</i>	0,02	3	0,016
<i>Ultrasound equipment</i>	0,75	10	2,047
<i>Zetasizer Nano Z</i>	0,01	2	0,005
<i>Contact Angle</i>	0,10	4	0,109
<i>FTIR spectrophotometer</i>	0,05	2	0,027
<i>Incubator 37 °C</i>	0,30	168	13,759
<i>Multiwell plate reader</i>	0,05	20	0,273
<i>Fluorescence Microscope</i>	0,09	10	0,246
<b>TOTAL</b>			<b>16,484</b>

Figure 30. The amounts of carbon dioxide generated during the process.

As a result, a total of 16,484 kg of the carbon dioxide has been generated during the process.

## 7. Conclusions

Herein, stable CGNPs with proved antibacterial activity were previously prepared by a green synthetic method without the utilization of harsh chemicals or energy-consuming processes and then enzymatically grafted with antifouling zwitterions on silicone surface in a one-pot laccase/high intensity ultrasound process. At first, silicone material was plasma-activated and preaminated with (3-aminopropyl)triethoxysilane (APTES), allowing subsequent laccase-catalyzed grafting of the CGNPs. Subsequently, the tethered phenolic residues from the CGNPs were activated by laccases to phenoxy radicals, triggering an sono-enzymatically initiated radical polymerization of zwitterionic sulfobetaine methacrylate monomers on the silicone catheters. The chemical groups and wettability properties were characterized by FTIR and water contact angle. The engineered hybrid coating showed increased hydrophilicity and reduced protein adsorption, important parameters governing the initial steps of sessile bacterial growth on indwelling medical devices. These coating composed of CGNPs and zwitterions completely inhibited the growth of *S. aureus* and *E. coli* planktonic cells and reduced the biofilm formation on silicone material by 80 %. Further durability tests under dynamic conditions in an *in vitro* model simulating the real application scenario of urinary catheters and cytotoxicity evaluation should be pursued to validate the potential of the these nanocoating for prevention of biofilm-associated infections.

## 8. Economic analysis

The economic study of the project has been divided between the equipment used and the staff. Each case has resulted in the total following costs:

Sector	Cost
Reagents and products	125,80 €
Equipment and material	873,65 €
Staff	5.856,48 €
<b>TOTAL:</b>	<b>6.855,93 €</b>

Figure 31. Table of the resulting costs of each proposed section, plus the total cost of the experimental nanoparticle coating process.

The total value is considered without taking into account water and electricity expenses.

### 8.1. Reagents and products

The costs of each component used in the experimental process has been calculated by the fraction used respectively:

Experimental Compounds	Capacity	Price	Fraction used	Cost
<i>DMSO</i>	1 L	59,01	0,005	0,30
<i>Lauryl Gallate</i>	50 g	99,70	0,012	1,20
<i>Tween 80</i>	500 ml	52,04	0,002	0,11
<i>Ethanol</i>	50 ml	80,10	0,600	48,06
<i>Sulfobetaine</i>	5 g	152,00	0,168	25,53
<i>Sodium Acetate</i>	250 g	29,80	0,002	0,06
<i>Sodium Carbonate</i>	500 g	25,40	0,001	0,03
<i>Folin-Ciocalteu</i>	100 ml	47,60	0,100	4,76
<i>Fluorescamine</i>	100 mg	158,00	0,036	5,69



<i>Crystal Violet</i>	25 g	77,30	0,001	0,08
<i>Resazurin</i>	1 g	37,50	0,100	3,75
<i>DPPH</i>	1 g	129,00	0,005	0,65
<i>FTIC-BSA</i>	5 mg	272,00	0,100	27,20
<i>Live/Dead</i>	5 ml	838,00	0,01	8,38
<b>TOTAL</b>				125,8

Figure 32. Table of the different compounds used for this experimental process with their prices and sales quantities. The cost proportional to the used fraction of each one has been calculated.

## 8.2. Equipment and material

In this research it has been possible to develop the coating and the nanoparticles of the project with all the equipment available to GBMI, without the need to rent the facilities of any laboratory, except for the realization of the SEM:

Equipment and material	Time (h)	Lotte	Price (€/ut)	Fraction used	Cost (€)
<i>SEM</i>	5	-	106,70	-	533,50
<i>96-well plate</i>	-	25	106,24	2,00	212,48
<i>Eppendorf (1,5ml)</i>	-	200	44,91	1,00	44,91
<i>Falcon (15ml)</i>	-	500	411,00	0,14	57,54
<i>Pipette tip (200µl)</i>	-	1000	27,65	0,40	11,06
<i>Pipette tip (1000µl)</i>	-	1000	70,80	0,20	14,16
<b>TOTAL</b>					873,65

Figure 33. Table of costs of the material and equipment required to carry out each of the assays and synthesis.

### 8.3. Staff

The overall cost of the working time has been approached as an internship, accounting for the hourly rate of 8 euros plus the 2% withholding tax.

Activity	Time (h)	Cost (€/h)	Worth (€)
Experimental work	540	8	4.320
Research	67	8	536
Analysis of results	140	8	1.120
Gross wage			5.976
Total wage			5.856,48

Figure 34. Table about the overall cost of working time, including experimental work and its subsequent analysis, such as bibliography research

## 9. Reference

- [1] G. Ferreres, K. Ivanova, J. Torrent-Búrgués y T. Tzanov, «Multimodal silver-chitosan-acylase nanoparticles inhibit bacterial growth and biofilm formation by Gram-negative *Pseudomonas aeruginosa* bacterium,» *ELSEVIER*, pp. 576-586, 2023.
- [2] G. Ferreres, K. Ivanova, I. Ivanov y T. Tzanov, «Nanomaterials and Coatings for Managing Antibiotic-Resistant Biofilms,» *Antibiotics*, p. 18, 2023.
- [3] J. O'Neil, «Tackling Drug - Resistant Infections Globally: Final Report and Recommendations,» Review Antimicrobial Resistance, 2016.
- [4] S. Joanna Chmielewska, K. Sklodowski, J. Depciuch, P. Deptula, E. Piktel, K. Fiedoruk, M. Parlinska-Wojtan, P. B Savage y R. Bucki, «Bactericidal Properties of Rod-, Peanut-, and Star-Shaped Gold Nanoparticles Coated with Ceragenin CSA-131 against Multidrug-Resistant Bacterial Strains,» *Pharmaceutics*, p. 27, 2021.
- [5] M. Polívková, T. Hubáček, M. Staszek, V. Svorcik y J. Siegel, «Antimicrobial Treatment of Polymeric Medical Devices by Silver Nanomaterials and Related Technology,» *Molecular Sciences*, p. 18, 2017.
- [6] A. Ivanova, K. Ivanova y T. Tzanov, «Simultaneous Ultrasound-Assisted Hybrid Polyzwitterion/Antimicrobial Peptide Nanoparticles Synthesis and Deposition on Silicone Urinary Catheters for Prevention of Biofilm-Associated Infections,» *Nanomaterials*, pp. 1-12, 2021.
- [7] C. Desrousseaux, V. Sautou, S. Descamps y O. Traoré, «Modification of the surfaces of medical devices to prevent microbial adhesion and biofilm formation,» *ELSEVIER*, pp. 87-93, 2013.
- [8] S. G. y. C. V. Preuss, «Pharmacokinetics,» *StatPearls*, 2022.
- [9] O. Salata, «Applications of nanoparticles in biology and medicine.,» *J Nanobiotechnology*, 2004.
- [10] S. Grogan y C. V. Preuss, «Pharmacokinetics,» *StatPearls*, 2022.
- [11] O. Salata, «Applications of nanoparticles in biology and medicine,» *J Nanobiotechnology*, 2004.

- [12] M. Jaiswal, R. Dudhe y P. Sharma, «Nanoemulsion: an advanced mode of drug delivery system,» *3 Biotech*, pp. 123-127, 2015.
- [13] K. I. J. T.-B. a. T. T. G. Ferreres, "Multimodal silver-chitosan-acylase nanoparticles inhibit bacterial growth and biofilm formation by Gram-negative *Pseudomonas aeruginosa* bacterium," *Elsevier*, vol. 646, pp. 576-586, 2022.
- [14] A. B. M. N. G. J. E. B. a. T. T. A. Gala Morena, "Antibacterial Properties and Mechanisms of Action of Sonoenzymatically Synthesized Lignin-Based Nanoparticles," *Applied Materials & Interfaces*, pp. 37270-37279, 2022.
- [15] K. I. I. I. a. T. T. G. Ferreres, «Nanomaterials and Coatings for Managing Antibiotic-Resistant Biofilms.,» *Antibiotics*, pp. 1-18, 2023.
- [16] «Factor de emisión de la energía eléctrica: el mix eléctrico.,» 2023. [En línea]. Available: [https://canviclimatic.gencat.cat/es/actua/factors\\_demissio\\_associats\\_a\\_lenergia/](https://canviclimatic.gencat.cat/es/actua/factors_demissio_associats_a_lenergia/).

